Eur Respir J 2009; 34: 1159–1166
DOI: 10.1183/09031936.00195708

All-*trans*-retinoic acid inhibits tumour growth of malignant pleural mesothelioma in mice

C. Tabata*, R. Tabata#, N. Hirayama*, A. Yasumitsu*, S. Yamada*, A. Murakami*, S. Iida*, K. Tamura*, T. Terada*, K. Kuribayashi*, K. Fukuoka* and T. Nakano*

ABSTRACT: **Malignant pleural mesothelioma (MPM) is an aggressive malignant tumour of mesothelial origin associated with asbestos exposure. Because MPM has limited response to conventional chemotherapy and radiotherapy, the prognosis is very poor. Several researchers have reported that cytokines such as interleukin (IL)-6 play an important role in the growth of MPM. Previously, it was reported that all-*trans*-retinoic acid (ATRA) inhibited the production and function of IL-6 and transforming growth factor (TGF)-β1 in experiments using lung fibroblasts.**

We investigated whether ATRA had an inhibitory effect on the cell growth of MPM, the origin of which was mesenchymal cells similar to lung fibroblasts, using a subcutaneous xenograft mouse model. We estimated the tumour growth and performed quantitative measurements of IL-6, TGF-β1 and platelet-derived growth factor (PDGF) receptor (PDGFR)-β mRNA levels both of cultured MPM cells and cells grown in mice with or without the administration of ATRA.

ATRA significantly inhibited MPM tumour growth. *In vitro* studies disclosed that the administration of ATRA reduced 1) mRNA levels of TGF-β1, TGF-β1 receptors and PDGFR-β, and 2) TGF-β1-dependent proliferation and PDGF-BB-dependent migration of MPM cells.

These data may provide a rationale to explore the clinical use of ATRA for the treatment of MPM.

KEYWORDS: **Cytokines, mesothelioma**

Malignant pleural mesothelioma (MPM) is an aggressive malignant tumour of mesothelial origin associated with asbestos exposure [1]. Although recently asbestos usage has decreased throughout the world, the incidence of MPM is expected to markedly increase over the next few decades because there is a long latency period (20–40 yrs) between asbestos exposure and tumour development [2]. MPM has limited response to conventional chemotherapy and radiotherapy, so the prognosis is very poor, with median survival durations of 8–18 months [3]. Despite much research into MPM treatment, there has been little progress in effective therapeutic and preventive strategies against MPM, and the development of novel treatment is urgently needed [4].

According to recent research investigating cytokines in relation to MPM, several cytokines, such as interleukin (IL)-6 [5] and hepatocyte growth factor/scatter factor [6], play an important role in the growth of MPM.

All-*trans*-retinoic acid (ATRA), a physiological metabolite of vitamin A, is known to affect cell differentiation, proliferation and development. ATRA has been widely used in differentiation therapy for acute promyelocytic leukaemia (APL) with the ability to overcome promyelocytic leukaemia/retinoic acid receptor fusion protein. There have been several reports about the effects of ATRA on cytokine production [7–9]. ATRA induced the growth inhibition of myeloma cells, which proliferated in IL-6 autocrine and paracrine manners, with the reduction of both IL-6 production and its receptor (IL-6R) expression [10, 11]. In a previous report, it was demonstrated that ATRA reduced irradiation-induced proliferation of lung fibroblasts by inhibiting both IL-6 production and IL-6R expression [12]. Moreover, it was recently reported that ATRA prevented both irradiation- and bleomycin-induced pulmonary fibrosis in mice *via* an inhibitory effect on both IL-6-dependent fibroblast proliferation and transforming growth factor (TGF)-β1-dependent transdifferentiation of fibroblasts into myofibroblasts [13].

In the present study, we investigated whether ATRA had an inhibitory effect on the cell growth of MPM, the origin of which was mesenchymal cells similar to lung fibroblasts and associated with several cytokines, including IL-6.

METHODS

Cell culture

Human MPM cell lines H28 (epithelioid), H2052 (sarcomatoid), H2452 (biphasic) and MSTO-211H

AFFILIATIONS
*Division of Respiratory Medicine, Dept of Internal Medicine, Hyogo College of Medicine, Nishinomiya, and
#Dept of Internal Medicine, Hyogo Prefectural Tsukaguchi Hospital, Amagasaki, Japan.

CORRESPONDENCE
C. Tabata
Division of Respiratory Medicine,
Dept of Internal Medicine
Hyogo College of Medicine
1-1 Mukogawa-cho
Nishinomiya
Hyogo
663-8501 Japan
E-mail: ctabata@hyo-med.ac.jp

Received:
Dec 24 2008
Accepted after revision:
April 08 2009
First published online:
May 14 2009

European Respiratory Journal
Print ISSN 0903-1936
Online ISSN 1399-3003

(biphasic) and human mesothelial cell line MeT-5A were obtained from the American Type Culture Collection (Rockville, MD, USA). These cells were cultured in RPMI 1640 (Sigma Chemical Co., St Louis, MO, USA) supplemented with 10% heat-inactivated fetal calf serum. ATRA (Sigma) was added to the growth medium to yield the final dimethyl sulfoxide (DMSO) solvent concentration <0.05% (v/v). In some experiments, the cells were pre-incubated with proteasome inhibitor MG-132 (5 μM) [14], Jun N-terminal kinase (JNK) inhibitor SP600125 (10 μM) [15], p38 mitogen-activated protein kinase (MAPK) inhibitor SB203580 (10 μM) [16] or extracellular signal-regulated kinase (ERK)1/2 inhibitor PD98059 (25 μM) [13] for 60 min (all Calbiochem, San Diego, CA, USA).

Animals

6-week-old C.B-17/Icr-*scid* Jcl (*scid/scid*) (SCID) female mice were purchased from Clea Japan (Tokyo, Japan) and maintained in our specific pathogen-free animal facility. All animals were kept according to the Animal Protection Guidelines of Hyogo College of Medicine (Hyogo, Japan). All protocols for animal use and euthanasia were reviewed and approved by the Institute of Laboratory Animals, Graduate School of Medicine, Hyogo College of Medicine.

Ectopic (subcutaneous) xenograft model

To produce subcutaneous (*s.c.*) tumours, a single-cell suspension of 10^7 MSTO-211H cells was implanted *s.c.* into the back of SCID mice. In some experiments, mice were injected intraperitoneally with 0.5 mg of ATRA dissolved in 0.1 mL cottonseed oil or with 0.1 mL cottonseed oil alone (controls). Injections were repeated three times weekly, 1) throughout the course, or 2) in the latter half of the period from inoculation to the end of the observation period. In previous studies, 0.5 mg of ATRA administration three times per week for 6 months did not produce noticeable morbidity and mortality [12, 13]. The tumours were measured every 7 days with calipers, and their volumes were calculated using the formula $a(b^2)/2$, in which a and b represent the longest and shortest diameters, respectively.

Quantitative real-time reverse transcriptase PCR

Total RNA was isolated by RNeasy Mini kit (QIAGEN, Valencia, CA, USA), and reverse-transcribed by High Capacity cDNA Reverse Transcription Kit (Applied Biosystems, Foster City, CA, USA). Quantitative real-time reverse transcriptase (RT)-PCR was performed as previously described [12, 13], using TaqMan Gene expression products for human IL-6, IL-6R, TGF-β1, TGF-β1 receptor (TGF-β1R) type 1, TGF-β1R type 2, platelet-derived growth factor (PDGF)-β, PDGF receptor (PDGFR)-β and cytochrome gene CYP26A1. 18S ribosomal (r)RNA served as an endogenous control (Applied Biosystems).

Measurement of nuclear factor-κB p65, p38MAPK and JNK

Nuclear extracts were prepared and protein concentration in nuclear extracts was measured as previously described [12]. Nuclear factor (NF)-κB p65, cytoplasmic phospho-p38MAPK ($pThr^{180}/pThr^{182}$) and cytoplasmic JNK were detected by ELISA Kit (BioSource (Camarillo, CA, USA), Sigma and Active Motif (Carlsbad, CA, USA), respectively).

Cell proliferation assay

Cell proliferation assays were performed as previously described [12]. Cells were cultured in 96-well flat-bottomed culture plates for 2 days with or without TGF-β1 (1–10,000 $pg \cdot mL^{-1}$), and/or ATRA (10^{-5} M).

Cell migration assay

In vitro migration assays were performed by CytoSelect 24-well Cell Migration Assay (8 μm, Colorimetric Format; CELL BIOLABS, Huissen, the Netherlands), according to the manufacturer's instructions. Briefly, MSTO-211H cells were pre-cultured overnight with or without ATRA (10^{-5} M) and were then suspended at a density of 1×10^6 $cells \cdot mL^{-1}$ in RPMI 1640 and placed in the upper half of the Boyden chamber. The lower half of the Boyden chamber was filled with RPMI 1640 containing 10 $ng \cdot mL^{-1}$ human recombinant PDGF-BB (PeproTech, London, UK) or RPMI 1640 alone.

Analysis of apoptosis

MPM cells undergoing apoptosis were detected in tissue sections by the terminal deoxynucleotidyl transferase-mediated deoxyuridine triphosphate-biotin nick-end labelling (TUNEL) method, using the *in situ* apoptosis detection TUNEL kit (Takara, Shiga, Japan) according to the manufacturer's instructions.

Statistical analysis

The results are given as the mean±SD of three experiments performed in triplicate. Statistical analysis was performed using the Bonferroni/Dunn multiple comparisons test. In all tests, a p-value <0.05 was considered significant.

RESULTS

Inhibitory effect of ATRA on proliferation of MPM cells

We first investigated the effect of ATRA on the growth of both MPM (H28, H2052, H2452 and MSTO-211H) and mesothelial (MeT-5A) cells. Cells were cultured with or without various concentrations of ATRA for 48 h. The addition of ATRA had a suppressive effect on the proliferation of all of these MPM cells in a dose-dependent manner. The maximum inhibitory effect was observed at the concentration of 10^{-5} M ATRA (H28: 59% decrease ($p<0.0001$); H2042: 33% decrease ($p<0.0001$); H2452: 45% decrease ($p<0.0001$); MSTO-211H: 29% decrease ($p<0.0001$)) (fig. 1a–d), whereas the lower concentrations (10^{-7} M or 10^{-6} M) of ATRA showed a minor effect compared with 10^{-5} M. Conversely, ATRA had no effect on the proliferation of MeT-5A (fig. 1e). The final concentration of DMSO (0.05% v/v) had no gross effect on any cells (data not shown). The concentration of 10^{-5} M ATRA had no effect on cell viabilities in any cell lines (data not shown).

Effect of ATRA on TGF-β1/TGF-β1R mRNA expression of MPM cells

As shown in figure 2a, the TGF-β1 mRNA as a ratio of 18S rRNA expression was decreased following 7 h of culture with 10^{-5} M ATRA: by 29% in H28 ($p<0.0001$), by 47% in H2052 ($p=0.0002$), by 38% in H2452 ($p=0.0002$) and by 56% in MASTO-211H cells ($p<0.0001$), compared with cells incubated with DMSO alone. Conversely, ATRA had no effect on TGF-β1 mRNA expression in MeT-5A mesothelial cells. Both TGF-β1R type 1 and type 2 mRNA/18S rRNA ratios were also decreased with ATRA

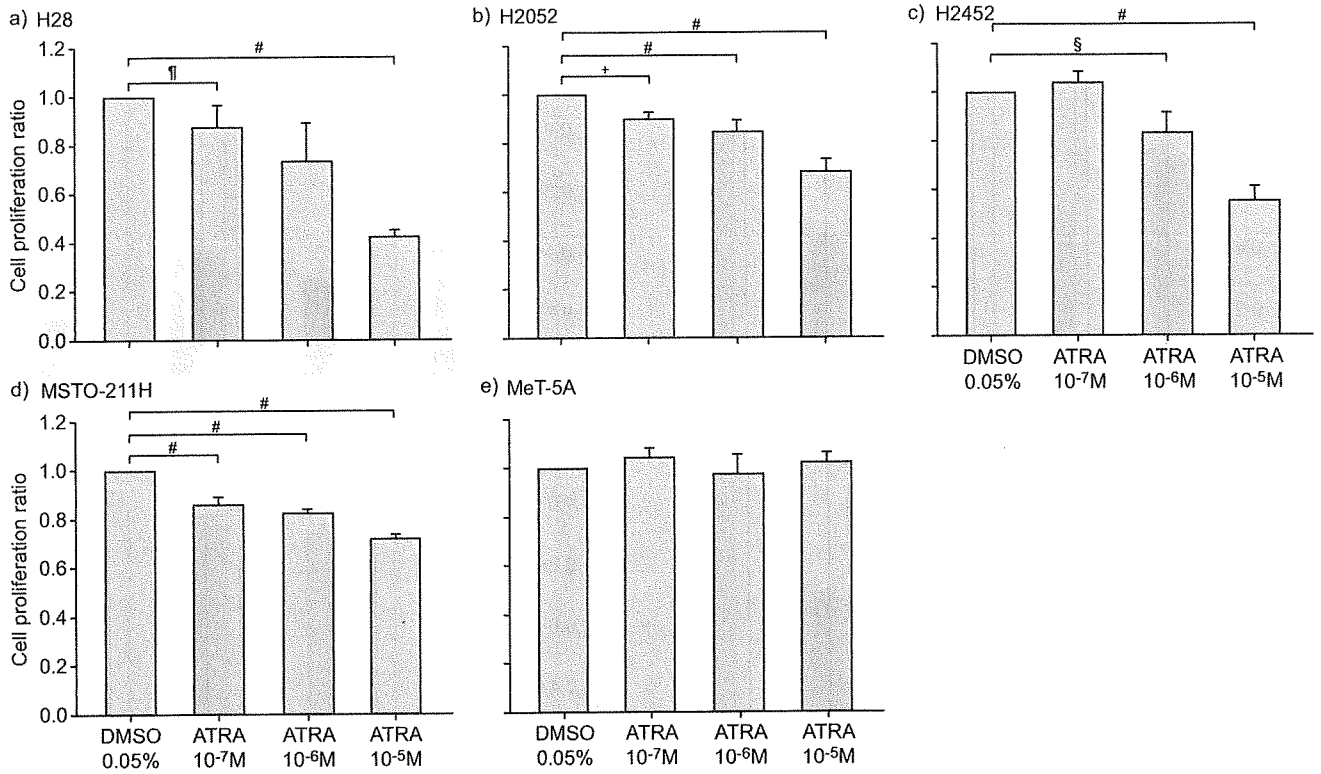

FIGURE 1. Inhibitory effect of all-*trans*-retinoic acid (ATRA) on proliferation of malignant pleural mesothelioma (MPM) cells. a) H28, b) H2052, c) H2452 and d) MSTO-211H MPM cells and e) human mesothelial cell line MeT-5A were cultured in 96-well flat-bottomed culture plates for 48 h in serum-free medium with or without (dimethyl sulfoxide (DMSO) alone) various concentrations (10^{-7}, 10^{-6} or 10^{-5} M) of ATRA, and cell proliferation was assayed. The results are indicated as the mean±SD of three separate experiments in triplicate. #: $p<0.0001$; ¶: $p=0.0005$; +: $p=0.0035$; §: $p=0.0026$.

compared with cells incubated with DMSO alone (type 1: 19% in H28 ($p=0.0023$), 22% in H2052 ($p<0.0001$), 29% in H2452 ($p<0.0001$) and 42% in MSTO-211H ($p<0.0001$); type 2: 48% in H28 ($p<0.0001$), 27% in H2052 ($p=0.0003$), 43% in H2452 ($p<0.0001$) and 57% in MSTO-211H ($p<0.0001$). Conversely, ATRA had no effect on TGF-β1R type 1 and type 2 mRNA expression in MeT-5A (fig. 2b and c).

Involvement of NF-κB in the suppressive effect of ATRA on TGF-β1 mRNA expression

Proteasome inhibitor MG-132 is also known to have an inhibitory effect on NF-κB activity. Pretreatment of MPM cells with MG-132 led to decreased TGF-β1 mRNA levels by 47% in H28 ($p<0.0001$), 68% in H2052 ($p<0.0001$), 60% in H2452 ($p<0.0001$) and 75% in MSTO-211H ($p<0.0001$) compared with cells incubated with DMSO alone (fig. 3a). Next, we demonstrated that the levels of nuclear NF-κB p65 in these cells were suppressed in the presence of ATRA by 11% in H28 ($p=0.0162$), 13% in H2052 ($p=0.018$), 10% in H2452 ($p=0.0302$) and 14% in MSTO-211H ($p=0.0012$) compared with cells incubated with DMSO alone (fig. 3b). Although pretreatment with inhibitors for both p38MAPK and JNK led to decreased TGF-β1 mRNA levels in these cells, the level of phospho-p38MAPK and activity of JNK were not affected by ATRA (data not shown). Inhibitors of ERK1/2 had no effect on TGF-β1 mRNA levels (data not shown).

Effect of ATRA on TGF-β1-mediated proliferation of MPM cells

To clarify the involvement of TGF-β1 in the development of MPM tumour growth, we studied the effect of TGF-β1 on the proliferation of MPM cells and MeT-5A mesothelial cells. As shown in figure 4a, the addition of TGF-β1 stimulated all MPM cell growth in a dose-dependent manner and reached a plateau at the concentration of 1,000 $pg \cdot mL^{-1}$ (H28: 18% increase ($p=0.0012$); H2042: 19% increase ($p=0.0015$); H2452: 30% increase ($p<0.0001$); MSTO-211H: 46% increase ($p=0.0069$)). Conversely, TGF-β1 had no effect on the proliferation of MeT-5A mesothelial cells (fig. 4a). We then evaluated the effect of ATRA on TGF-β1-mediated proliferation of MPM cells, and showed that the TGF-β1-mediated proliferation was decreased with ATRA by 39% in H28 ($p<0.0001$), 48% in H2052 ($p=0.0013$), 80% in H2452 ($p<0.0001$) and 73% in MSTO-211H ($p<0.0001$) compared with cells incubated with DMSO alone (fig. 4b).

Antitumour efficacy of ATRA in a subcutaneous xenograft model

We next examined the effect of ATRA on a *s.c.* xenograft mouse model of MPM cells. A single-cell suspension of 10^7 H28, H2052, H2452 and MSTO-211H cells with a viability of >95% was implanted *s.c.* into the back of SCID mice. Only MSTO-211H cells could grow on the back of SCID mice. To study the

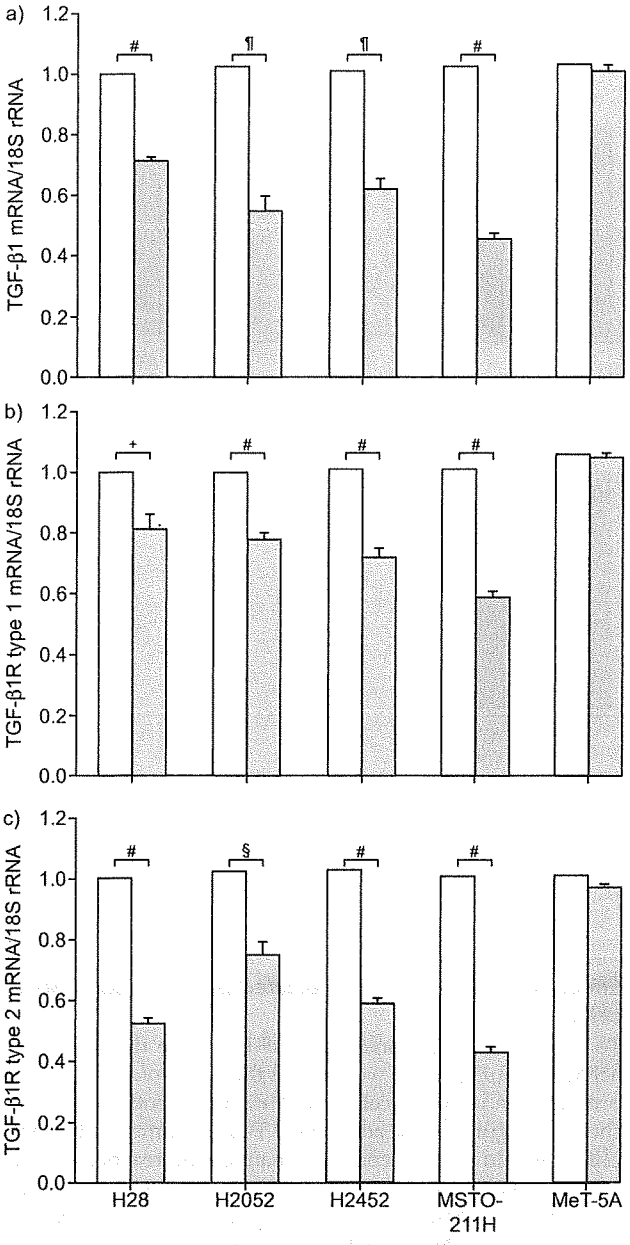

FIGURE 2. Effect of all-*trans*-retinoic acid (ATRA) on transforming growth factor (TGF)-β1/TGF-β1 receptor (TGF-β1R) mRNA expression of malignant pleural mesothelioma (MPM) cells. Real-time reverse transcriptase PCR was performed to determine the changes in mRNA levels for TGF-β1/TGF-β1Rs. H28, H2052, H2452 and MSTO-211H MPM cells and the human mesothelial cell line MeT-5A were cultured in the presence (▒) or absence (dimethyl sulfoxide (DMSO) alone; □) of 10^{-5} M of ATRA for 7 h. The levels of mRNA for a) TGF-β1, b) TGF-β1R type 1 and c) TGF-β1R type 2 are represented as the ratio to 18S ribosomal (r)RNA, an endogenous control. The results are indicated as the mean±SD of three separate experiments in triplicate. #: p<0.0001; ¶: p=0.0002; +: p=0.0023; §: p=0.0003.

"preventive" and "therapeutic" effects of ATRA on MSTO-211H cell growth, *i.p.* injections of ATRA were repeated three times weekly, 1) throughout the course, or 2) in the latter half of the period from inoculation to the end of the observation period. As shown in figure 5a, *i.p.* administration of ATRA

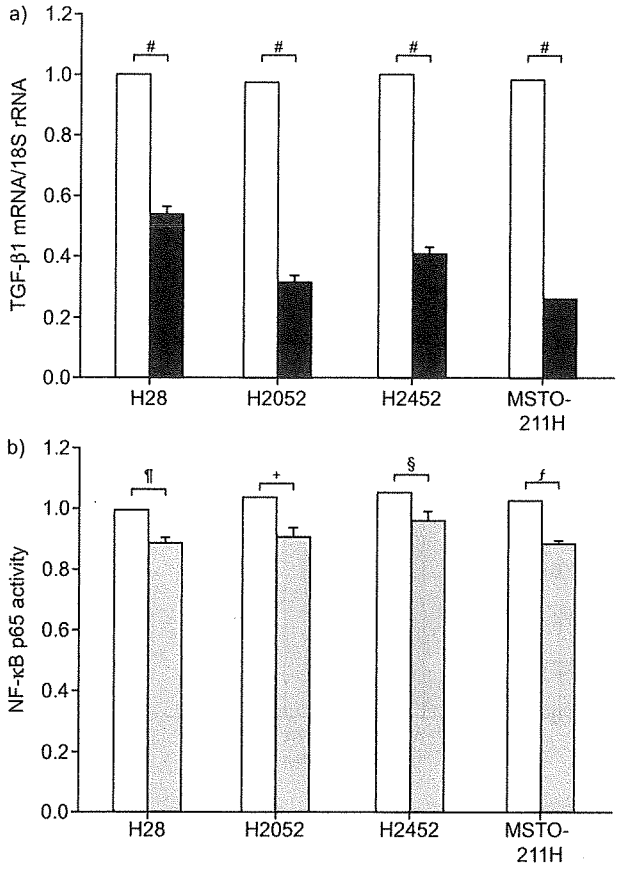

FIGURE 3. Involvement of nuclear factor (NF)-κB in the suppressive effect of all-*trans*-retinoic acid (ATRA) on transforming growth factor (TGF)-β1 mRNA expression. a) H28, H2052, H2452 and MSTO-211H malignant pleural mesothelioma cells were cultured in the presence (▒) or absence (dimethyl sulfoxide (DMSO) alone; □) of 5 μM MG-132 for 7 h. Real-time reverse transcriptase PCR was performed to determine changes in TGF-β1 mRNA levels. b) The activities of NF-κB were analysed. H28, H2052, H2452 and MSTO-211H cells were treated with (▒) or without (DMSO alone; □) ATRA (10^{-5} M) for 1 h and NF-κB p65 amounts in nuclear protein extracts were analysed. The results are indicated as the mean±SD of three separate experiments in triplicate. #: p<0.0001; ¶: p=0.0162; +: p=0.018; §: p=0.0302; ƒ: p=0.0012.

three times per week throughout the course greatly inhibited tumour growth at 28 days after inoculation (68% decrease; p<0.0001). Moreover, treatment with ATRA three times per week for the latter half of the period from inoculation to the end of the observation period ameliorated tumour growth better than the vehicle control group (36% decrease; p=0.0011). The *i.p.* injection with 0.5 mg of ATRA three times a week for 28 days had no effect on the health of the mice.

mRNA levels of TGF-β1 and PDGFR-β in implanted grown tumours on SCID mice

TGF-β1 mRNA levels of implanted grown MPM tumours on SCID mice at 28 days after inoculation with or without an *i.p.* injection of ATRA were analysed by real-time RT-PCR. We demonstrate in figure 5b that TGF-β1 mRNA expression was significantly suppressed by the administration of ATRA (32% decrease; p=0.0008). To study whether another mechanism

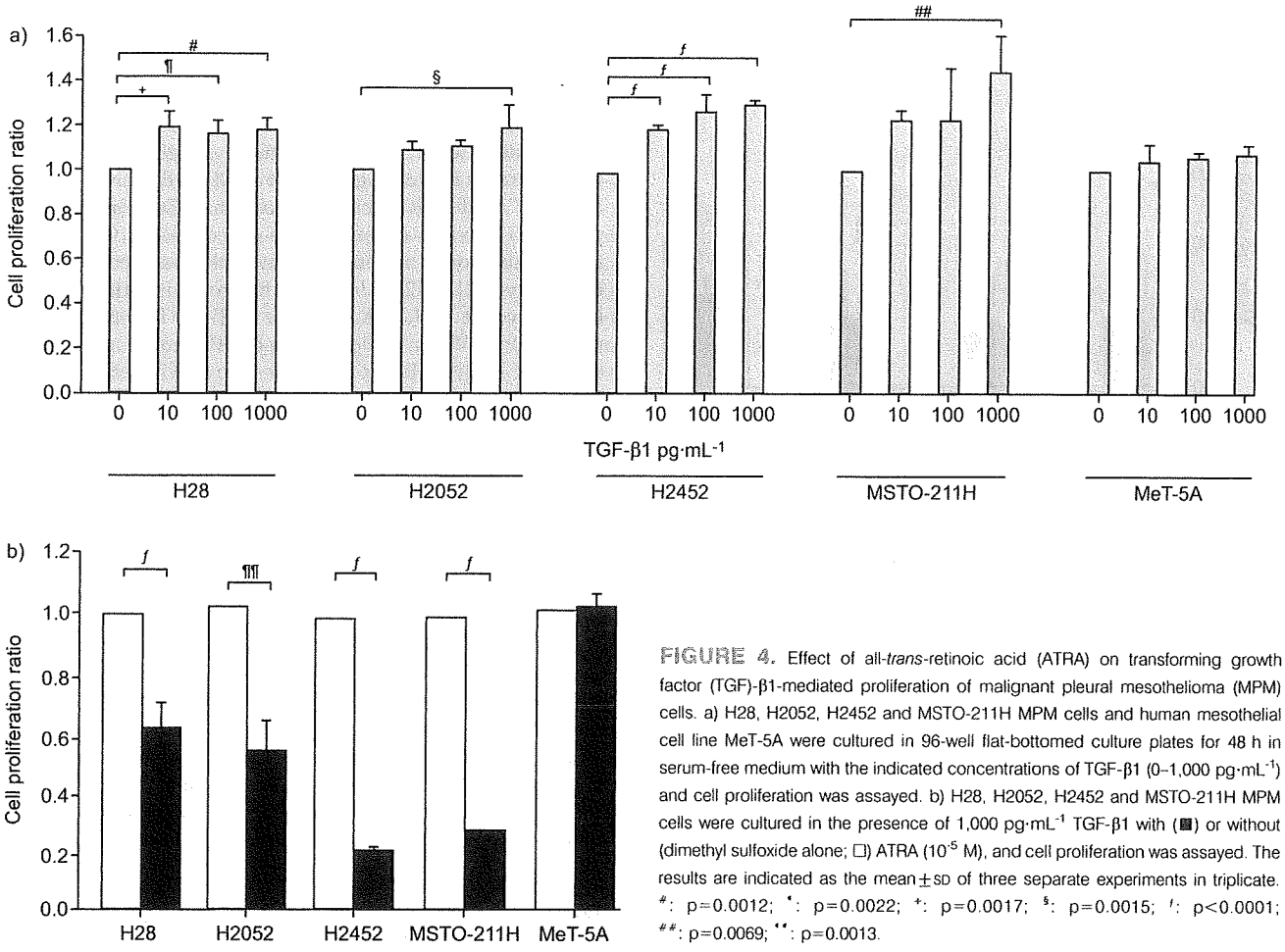

FIGURE 4. Effect of all-*trans*-retinoic acid (ATRA) on transforming growth factor (TGF)-β1-mediated proliferation of malignant pleural mesothelioma (MPM) cells. a) H28, H2052, H2452 and MSTO-211H MPM cells and human mesothelial cell line MeT-5A were cultured in 96-well flat-bottomed culture plates for 48 h in serum-free medium with the indicated concentrations of TGF-β1 (0–1,000 pg·mL^{-1}) and cell proliferation was assayed. b) H28, H2052, H2452 and MSTO-211H MPM cells were cultured in the presence of 1,000 pg·mL^{-1} TGF-β1 with (■) or without (dimethyl sulfoxide alone; □) ATRA (10^{-5} M), and cell proliferation was assayed. The results are indicated as the mean±SD of three separate experiments in triplicate. #: p=0.0012; ¶: p=0.0022; +: p=0.0017; §: p=0.0015; ƒ: p<0.0001; ##: p=0.0069; ¶¶: p=0.0013.

was involved in the preventive effect of ATRA on MPM tumour progression, we focused on previous reports demonstrating that human mesothelioma cell lines expressed PDGFR-β [17]. We then analysed PDGFR-β expression in implanted grown MPM tumours and found that, in mice treated with ATRA, the levels of PDGFR-β expression were markedly decreased as compared with mice without ATRA (31% decrease; p=0.0004; fig. 5c).

Inhibitory effect of ATRA on PDGFR-β expression and PDGF-BB-induced migration of MPM cells

We next examined the impact of ATRA on PDGFR-β mRNA expression in MPM cells. As shown in figure 6a, ATRA decreased the expression of PDGFR-β mRNA by 32% in MSTO-211H cells (p<0.0001); however, ATRA had no effect on the production of PDGF-BB (data not shown). It is well known that cell migration plays an important role in tumour cell invasion, especially in the wide spread of MPM tumours. We therefore performed an *in vitro* migration assay to study the effect of PDGF, which is a potent mitogen and chemotactic factor for several mesenchymal cells [18], on MPM progression, and revealed that MSTO-211H cell migration was induced (1.3 fold increase; p=0.0004) by PDGF-BB, which was inhibited in the presence of ATRA (19% decrease; p=0.0011; fig. 6b).

DISCUSSION

MPM is an aggressive malignant tumour of mesothelial origin associated with asbestos exposure that has limited response to conventional chemotherapy and radiotherapy; the prognosis is very poor. Recently, the multi-targeted anti-folate pemetrexed has been approved as a first-line agent in combination with cisplatin for the treatment of MPM; however, overall survival remains very poor [19].

It has previously been reported that ATRA prevented both irradiation- and bleomycin-induced pulmonary fibrosis in mice by the inhibition of both IL-6-dependent proliferation and TGF-β1-dependent transdifferentiation of lung fibroblasts. As MPM cells originate from mesenchymal cells similar to lung fibroblasts, here we examined the effect of ATRA on the progression of MPM tumour in SCID mice.

In the present study, we found that ATRA inhibited the proliferation of MPM cells but not mesothelial cells. Several factors, including IL-6, TGF-β1 and PDGF, have been reported to be associated with MPM cells [5, 6, 17, 20]. Here, we first examined whether the IL-6/IL-6R system also plays an important role in ATRA-mediated inhibition of MPM cell proliferation; however, in this study, ATRA had no effect on IL-6/IL-6R mRNA expression in MPM cells.

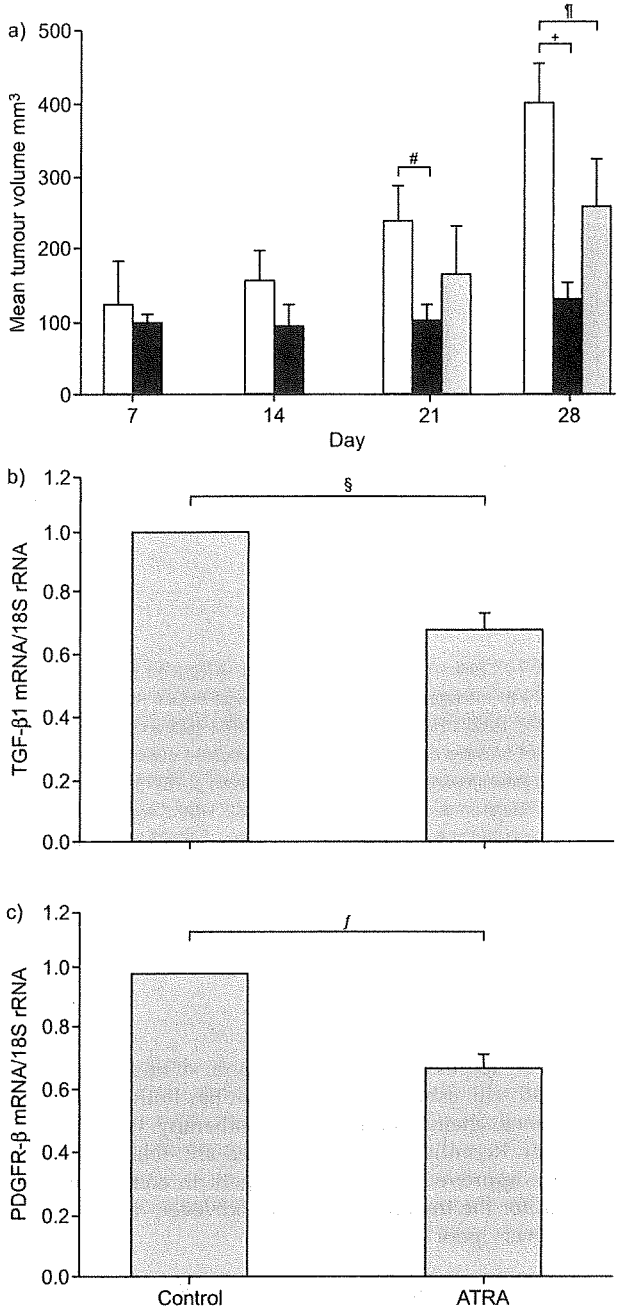

FIGURE 5. Antitumour efficacy with all-*trans*-retinoic acid (ATRA) in a subcutaneous xenograft model. MSTO-211H cells with a viability of >95% were implanted subcutaneously into the back of SCID mice. a) The tumours were measured and their volume calculated in mice treated with vehicle control (□), treated *i.p.* with ATRA three times per week throughout the course (day 0–28; ■) or in the latter half of the period from inoculation to the end of the observation period (day 14–28; ▒). b and c) Real-time reverse transcriptase PCR was performed to determine changes in mRNA levels in tumours for b) transforming growth factor (TGF)-β1 and c) platelet-derived growth factor receptor (PDGFR)-β. The levels of mRNA are the ratio to 18S ribosomal (r)RNA. The results are indicated as the mean±SD of three separate experiments in triplicate. #: p=0.0014; ¶: p=0.0011; +: p<0.0001; §: p=0.0008; ƒ: p=0.0004.

We then investigated the effect of ATRA on the production of TGF-β1, another key cytokine in ATRA-mediated inhibition of pulmonary fibrosis, as we have previously demonstrated. We here showed that ATRA suppressed mRNA expression of both TGF-β1 and TGF-β1R in these cells and, moreover, inhibited TGF-β1-dependent cell proliferation, suggesting that ATRA demonstrated the inhibitory effect on MPM cell proliferation *via* a TGF-β1/TGF-β1R autocrine mechanism. Generally, TGF-β1 is produced by various normal cells observed surrounding MPM tissues, including fibroblasts, macrophages, neutrophils and lymphocytes [21, 22]. *In vivo*, therefore, in addition to the inhibitory effect of ATRA *via* the TGF-β1/TGF-β1R autocrine mechanism, ATRA could decrease MPM tumour progression *via* the TGF-β1/TGF-β1R paracrine loop by MPM cells and these TGF-β1-producing surrounding cells. To determine the cellular mechanism in the regulation of TGF-β1 production of MPM cells, we used some well characterised pharmacological inhibitors [23]. There are at least three distinct MAPK signal transduction pathways in mammalian cells that lead to activation of the ERK, JNK and p38MAPK pathways. As the induction of most cytokine genes requires the activation of NF-κB, we next examined whether changes in NF-κB activity were involved in the suppressive effect of ATRA on TGF-β1 expression in MPM cells, and found an important role of NF-κB in this process (fig. 3). These results suggest a possible mechanism whereby ATRA could reduce TGF-β1 expression through an NF-κB-dependent pathway. Furthermore, it has been recently reported that the mechanism of asbestos-induced oncogenesis was associated with the activation of NF-κB [24], so the inhibitory effect of ATRA on NF-κB activation itself may be beneficial for the prevention of tumour growth in early MPM.

Next, we demonstrated in an *in vivo* study that *i.p.* administration of ATRA three times per week throughout the course greatly inhibited MPM tumour growth 28 days after inoculation. The administration of ATRA inhibited TGF-β1 mRNA expression in grown MPM tumours in SCID mice. A recent study reported that TGF-β1 was significantly associated with the growth of MPM cells in a murine MPM tumour model through TGF-β1/TGF-β1R systems and TGF-β1 signalling [25], and our study appears to support this.

It is well known that cell migration plays a pivotal role in the disease progression of cancer. PDGF acts as two types of peptide, A (16-kDa) and B (14-kDa) chains, with about 60% sequence identity, disulfide linked into three diametric molecules, PDGF-AA, -AB and -BB [26]. A and B chains bind to two cell-surface receptors: the α receptor can bind all three dimers (PDGF-AA, PDGF-AB and PDGF-BB) with high affinity and the β receptor can only recognise PDGF-BB with high affinity and PDGF-AB with lower affinity [27]. It has been previously reported that MPM cells express PDGF-α and PDGF-β mRNA, whereas no PDGF-β and a low level of PDGF-α mRNA expression are detected in normal mesothelial cells. Moreover, PDGFR-β mRNA expression is detected in MPM cells, whereas only PDGFR-α mRNA expression is observed in mesothelial cells [28]. In this study, we demonstrated that PDGFR-β mRNA expression in MPM cells was inhibited by ATRA (fig. 6a), while ATRA had no effect on PDGF-β mRNA expression (data not shown). Moreover, MPM cells migrated by PDGF-BB, which was suppressed by ATRA, as shown in figure 6b. PDGF-BB is also synthesised and

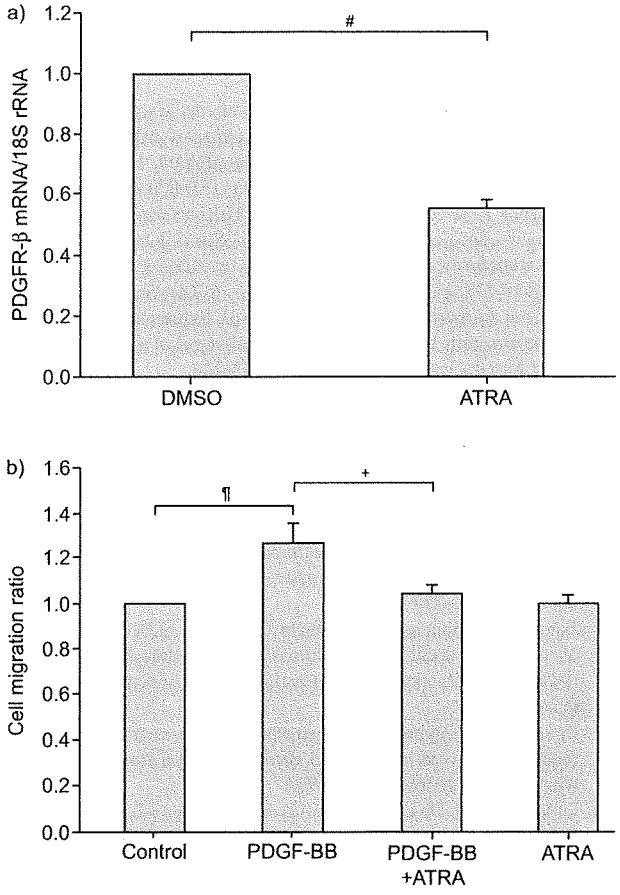

FIGURE 6. Inhibitory effect of all-*trans*-retinoic acid (ATRA) on platelet-derived growth factor (PDGF) receptor (PDGFR)-β expression and PDGF-BB-induced migration of malignant pleural mesothelioma (MPM) cells. a) Real-time reverse transcription PCR was performed to determine changes in mRNA levels for PDGFR-β. MSTO-211H MPM cells were cultured in the presence or absence (dimethyl sulfoxide (DMSO) alone) of 10^{-5} M of ATRA for 7 h. The levels of mRNA for PDGFR-β are the ratio to 18S ribosomal (r)RNA, an endogenous control. The results are indicated as the mean±SD of three separate experiments in triplicate. b) Cell migration assay. MSTO-211H cells were pre-cultured overnight with or without (DMSO alone) ATRA (10^{-5} M), and further cultured in the presence or absence of PDGF-BB (10 ng·mL^{-1}) with or without ATRA. The results are indicated as the mean±SD of three separate experiments in triplicate. #: $p<0.0001$; ¶: $p=0.0004$; +: $p=0.0011$.

released by several cells associated with MPM cells growth, such as fibroblasts, vascular smooth muscle cells and vascular endothelial cells [29]. The administration of ATRA had no effect on PDGF-β mRNA expression in MPM tumour cells grown on SCID mice in the present study. However, the reduction of PDGFR-β mRNA expression on MPM cells by ATRA may be estimated to inhibit the PDGF-BB/PDGFR-β paracrine loop of MPM cells and PDGF-BB-producing surrounding cells, which might increase MPM cell migration and tumour invasion in cases of human MPM. As for cell migration, it has been reported that retinoic acid inhibited fibronectin and laminin synthesis and cell migration of human pleural mesothelioma *in vitro* [30].

DE CUPIS *et al.* [31] demonstrated that fenretinide (4HPR), a synthetic derivative of retinoic acid, induced apoptosis of the MPM cell line ZL34. However, in their report, 4HPR induced apoptosis not only of tumour cells but also of MeT-5A, SV40-transformed normal mesothelial cells. Here, we demonstrate the selective inhibitory effect of ATRA on growth of MPM cells, but not of MeT-5A. By TUNEL assay, the increase of apoptosis was not observed in ATRA-treated MPM tumour cells in mice compared with untreated mice (data not shown). Next, we examined the mRNA expression of CYP26A1 [32], a retinoic acid regulated gene, by real-time RT-PCR, and found that mRNA levels of CYP26A1 were decreased in ATRA-treated MPM tumour cells in mice compared with untreated mice, which suggested an increased amount of active retinoic acid, namely, an autoregulation feedback loop (data not shown). However, it is not clear whether the observed effect is specific to retinoic acid signalling. Although the precise cellular mechanism has not been fully investigated, we propose the possibility that TGF-β1 and PDGF receptors play an important role in this mouse model and ATRA prevents MPM cell growth through the inhibition of these cytokine/cytokine receptor systems. Namely, we propose the dual inhibitory effect of ATRA on TGF-β1-dependent proliferation and PDGF-BB-dependent migration of MPM cells, which may be the mechanism underlying the preventive and therapeutic effect of ATRA on MPM.

It is noteworthy that in this report we showed the "late", *i.e.* "therapeutic", effect of ATRA in MPM cell growth (fig. 5a) in addition to the "throughout", *i.e.* "preventive", effect, because in clinical use, the therapeutic effect is often more important when clinicians find that MPM is already progressive in their patients.

ATRA is known to affect cell differentiation, proliferation and development. Clinically, ATRA has been widely used in differentiation therapy for APL [33]. Furthermore, oral administration of the drug results in good compliance. Our data may lead to the development of novel strategies incorporating ATRA for the prevention and treatment of MPM.

SUPPORT STATEMENT

Funding for the present study was received from KAKENHI, Grant-in-Aid for Scientific Research (C) (20590936) and Special Coordination Funds for Promoting Science and Technology (H18-1-3-3-1) (both Tokyo, Japan).

STATEMENT OF INTEREST

None declared.

ACKNOWLEDGEMENTS

We thank R. Morimoto and H. Kitai for technical assistance (both Division of Respiratory Medicine, Dept of Internal Medicine, Hyogo College of Medicine, Nishinomiya, Japan).

REFERENCES

1 Wagner JC, Sleggs CA, Marchand P. Diffuse pleural mesothelioma and asbestos exposure in the North Western Cape Province. *Br J Ind Med* 1960; 17: 260–271.

2 Selikoff IJ, Hammond EC, Seidman H. Latency of asbestos disease among insulation workers in the United States and Canada. *Cancer* 1980; 15: 2736–2740.

3 Nowak AK, Lake RA, Kindler HL, *et al.* New approaches for mesothelioma: biologics, vaccines, gene therapy, and other novel agents. *Semin Oncol* 2002; 29: 82–96.
4 Sterman DH, Kaiser LR, Albelda SM. Advances in the treatment of malignant pleural mesothelioma. *Chest* 1999; 116: 504–520.
5 Adachi Y, Aoki C, Yoshio-Hoshino N, *et al.* Interleukin-6 induces both cell growth and VEGF production in malignant mesotheliomas. *Int J Cancer* 2006; 119: 1303–1311.
6 Jagadeeswaran R, Ma PC, Seiwert TY, *et al.* Functional analysis of c-Met/hepatocyte growth factor pathway in malignant pleural mesothelioma. *Cancer Res* 2006; 66: 352–361.
7 Dubois C, Schlageter MH, de Gentile A, *et al.* Modulation of IL-8, IL-1β, and G-CSF secretion by all-*trans* retinoic acid in acute promyelocytic leukemia. *Leukemia* 1994; 8: 1750–1757.
8 Maeno T, Tanaka T, Sando Y, *et al.* Stimulation of vascular endothelial growth factor gene transcription by all *trans* retinoic acid through Sp1 and Sp3 sites in human bronchioloalveolar carcinoma cells. *Am J Respir Cell Mol Biol* 2002; 26: 246–253.
9 Pelicano L, Li F, Schindler C, *et al.* Retinoic acid enhances the expression of interferon-induced proteins: evidence for multiple mechanisms of action. *Oncogene* 1997; 15: 2349–2359.
10 Ogata A, Nishimoto N, Shima Y, *et al.* Inhibitory effect of all-*trans* retinoic acid on the growth of freshly isolated myeloma cells *via* interference with interleukin-6 signal transduction. *Blood* 1994; 84: 3040–3046.
11 Sidell N, Taga T, Hirano T, *et al.* Retinoic acid-induced growth inhibition of a human myeloma cell line *via* down-regulation of IL-6 receptors. *J Immunol* 1991; 146: 3809–3814.
12 Tabata C, Kubo H, Tabata R, *et al.* All-*trans* retinoic acid modulates radiation-induced proliferation of lung fibroblasts *via* IL-6/IL-6R system. *Am J Physiol Lung Cell Mol Physiol* 2006; 290: 597–606.
13 Tabata C, Kadokawa Y, Tabata R, *et al.* All-*trans*-retinoic acid prevents radiation- or bleomycin-induced pulmonary fibrosis. *Am J Respir Crit Care Med* 2006; 174: 1352–1360.
14 Jang BC, Jung TY, Paik JH, *et al.* Tetradecanoyl phorbol acetate induces expression of Toll-like receptor 2 in U937 cells: involvement of PKC, ERK, and NF-κB. *Biochem Biophys Res Commun* 2005; 328: 70–77.
15 Lee KY, Ito K, Hayashi R, *et al.* NF-κB and activator protein 1 response elements and the role of histone modifications in IL-1β-induced TGF-β1 gene transcription. *J Immunol* 2006; 176: 603–615.
16 Fritz DK, Kerr C, Tong L, *et al.* Oncostatin-M up-regulates VCAM-1 and synergizes with IL-4 in eotaxin expression: involvement of STAT6. *J Immunol* 2006; 176: 4352–4360.
17 Versnel MA, Claesson-Welsh L, Hammacher A, *et al.* Human malignant mesothelioma cell lines express PDGF β-receptors whereas cultured normal mesothelial cells express predominantly PDGF α-receptors. *Oncogene* 1991; 6: 2005–2011.
18 Ross R, Raines EW, Bowen-Pope DF. The biology of platelet-derived growth factor. *Cell* 1986; 46: 155–169.
19 Vogelzang NJ, Rusthoven JJ, Symanowski J, *et al.* Phase III study of pemetrexed in combination with cisplatin *versus* cisplatin alone in patients with malignant pleural mesothelioma. *J Clin Oncol* 2003; 21: 2636–2644.
20 Gerwin BI, Lechner JF, Reddel RR, *et al.* Comparison of production of transforming growth factor-β and platelet-derived growth factor by normal human mesothelial cells and mesothelioma cell lines. *Cancer Res* 1987; 47: 6180–6184.
21 Noble PW, Henson PM, Lucas C, *et al.* Transforming growth factor-β primes macrophages to express inflammatory gene products in response to particulate stimuli by an autocrine/paracrine mechanism. *J Immunol* 1993; 151: 979–989.
22 Derynck R, Jarrett JA, Chen EY, *et al.* Human transforming growth factor-β complementary DNA sequence and expression in normal and transformed cells. *Nature* 1985; 316: 701–705.
23 Sullivan DE, Ferris M, Pociask D, *et al.* Tumor necrosis factor-α induces transforming growth factor-β1 expression in lung fibroblasts through the extracellular signal-regulated kinase pathway. *Am J Respir Cell Mol Biol* 2005; 32: 342–349.
24 Yang H, Bocchetta M, Kroczynska B, *et al.* TNF-α inhibits asbestos-induced cytotoxicity *via* a NF-κB-dependent pathway, a possible mechanism for asbestos-induced oncogenesis. *Proc Natl Acad Sci USA* 2006; 103: 10397–10402.
25 Suzuki E, Kim S, Cheung HK, *et al.* A novel small-molecule inhibitor of transforming growth factor β type I receptor kinase (SM16) inhibits murine mesothelioma tumor growth *in vivo* and prevents tumor recurrence after surgical resection. *Cancer Res* 2007; 67: 2351–2359.
26 Betsholtz C, Johnsson A, Heldin CH, *et al.* cDNA sequence and chromosomal localization of human platelet-derived growth factor A-chain and its expression in tumour cell lines. *Nature* 1986; 320: 695–699.
27 Eriksson A, Siegbahn A, Westermark B, *et al.* PDGF α- and β-receptors activate unique and common signal transduction pathways. *EMBO J* 1992; 11: 543–550.
28 Langerak AW, De Laat PA, Van Der Linden-Van Beurden CA, *et al.* Expression of platelet-derived growth factor (PDGF) and PDGF receptors in human malignant mesothelioma *in vitro* and *in vivo*. *J Pathol* 1996; 178: 151–160.
29 Heldin CH, Westermark B. Mechanism of action and *in vivo* role of platelet-derived growth factor. *Physiol Rev* 1999; 79: 1283–1316.
30 Scarpa S, Giuffrida A, Palumbo C, *et al.* Retinoic acid inhibits fibronectin and laminin synthesis and cell migration of human pleural mesothelioma *in vitro*. *Oncol Rep* 2002; 9: 205–209.
31 de Cupis A, Semino C, Pirani P, *et al.* Enhanced effectiveness of last generation antiblastic compounds *vs.* cisplatin on malignant pleural mesothelioma cell lines. *Eur J Pharmacol* 2003; 473: 83–95.
32 Quere R, Baudet A, Cassinat B, *et al.* Pharmacogenomic analysis of acute promyelocytic leukemia cells highlights CYP26 cytochrome metabolism in differential all-*trans* retinoic acid sensitivity. *Blood* 2007; 109: 4450–4460.
33 Chen SJ, Zhu YJ, Tong JH, *et al.* Rearrangements in the second intron of the RARA gene are present in a large majority of patients with acute promyelocytic leukemia and are used as molecular marker for retinoic acid-induced leukemic cell differentiation. *Blood* 1991; 78: 2696–2701.

Expression of CUB domain containing protein (CDCP1) is correlated with prognosis and survival of patients with adenocarcinoma of lung

Jun-ichiro Ikeda,[1] Tomofumi Oda,[1,2] Masayoshi Inoue,[2] Takamasa Uekita,[3] Ryuichi Sakai,[3] Meinoshin Okumura,[2] Katsuyuki Aozasa[1] and Eiichi Morii[1,4]

Departments of [1]Pathology and [2]Thoracic Surgery, Osaka University Graduate School of Medicine, 2-2 Yamada-oka, Suita, Osaka, and [3]Growth Factor Division, National Cancer Center Research Institute, 5-1-1 Tsukiji, Chuo-ku, Tokyo, Japan

(Received September 29, 2008/Revised November 4, 2008/Accepted November 19, 2008/Online publication December 11, 2008)

CUB domain containing protein (CDCP1), a transmembrane protein with intracellular tyrosine residues which are phosphorylated upon activation, is supposed to be engaged in proliferative activities and resistance to apoptosis of cancer cells. Expression level of CDCP1 was examined in lung adenocarcinoma, and its clinical implications were evaluated. CDCP1 expression was immunohistochemically examined in lung adenocarcinoma from 200 patients. Staining intensity of cancer cells was categorized as low and high in cases with tumor cells showing no or weak and strong membrane staining, respectively. MIB-1 labeling index was also examined. There were 113 males and 87 females with median age of 63 years. Stage of disease was stage I in 144 cases (72.0%), II in 19 (9.5%), and III in 37 (18.5%). Sixty of 200 cases (30.0%) were categorized as CDCP1-high, and the remaining as CDCP1-low. Significant positive correlation was observed between CDCP1-high expression and relapse rate ($P < 0.0001$), poor prognosis ($P < 0.0001$), MIB-1 labeling index ($P < 0.0001$), and occurrence of lymph node metastasis ($P = 0.0086$). There was a statistically significant difference in disease-free survival (DFS) ($P < 0.0001$) and overall survival (OS) rates ($P < 0.0001$) between patients with CDCP1-high and CDCP1-low tumors. Univariate analysis showed that lymph node status, tumor stage, and CDCP1 expression were significant factors for both OS and DFS. Multivariate analysis revealed that only CDCP1 expression was an independent prognostic factor for both OS and DFS. CDCP1 expression level is a useful marker for prediction of patients with lung adenocarcinoma (*Cancer Sci* 2009; 100: 429–433).

Introduction

Since 1985 lung cancer has been the most common cause of cancer death in the world.[1] Non-small cell lung cancer (NSCLC) comprises 75–85% of all lung cancers, and approximately two-thirds of NSCLC patients have advanced stages at diagnosis. Despite the advances in the methods for detection and treatment of lung cancer, prognosis of NSCLC patients still remains unfavorable. Therefore, it is important to clarify the mechanism of tumor biology, and establishment of effective therapeutic modalities is essential to improve the prognosis in NSCLC. Previous studies accumulated information regarding the factors influencing prognosis in NSCLC. They include clinical, pathological, and molecular factors.

CUB domain containing protein (CDCP1) was originally identified as an epithelial tumor antigen by comparisons of molecules expressed in lung cancer cell lines and normal lung tissues.[2] CDCP1 is a transmembrane protein with three extracellular CUB domains, which are important for cell–cell interactions, and intracellular tyrosine residues which are phosphorylated upon activation.[2–7] Previously, we reported the epigenetic regulation of CDCP1 expression in the cell lines derived from various malignancies and clinical samples of breast cancer.[8,9] The CDCP1 expression level correlated with proliferative activities of breast cancer cells in the clinical samples.[8] Very recently, CDCP1 was reported to protect cells from anoikis, a form of apoptosis triggered by the loss of cell survival signals generated from interaction of cells with the extracellular matrix.[10] The knocked-down expression of CDCP1 by RNA interference abolished *in vitro* colony formation and *in vivo* metastatic abilities of lung adenocarcinoma cell line A549.[10] These findings showed that CDCP1 is required for protection of cells from anoikis, and suggest an important role of CDCP1 for tumorigenesis and metastasis, at least in cell lines. In the present study, CDCP1 expression was immunohistochemically examined in clinical samples from lung adenocarcinoma, and its clinical implications were evaluated.

Materials and Methods

Patients and tissue samples. Two hundred patients who underwent surgery for lung adenocarcinoma at Osaka University Hospital during the period from January 1993 to January 2004 were examined. Clinicopathological findings in these 200 patients are summarized in Table 1. There were 113 men and 87 women with ages ranging from 33 to 82 years (median, 63). Resected specimens were macroscopically examined to determine the location and size of the tumors. The size of the main tumor ranged from 8 to 70 mm (median, 24.5). The histological stage was determined according to the 6th edition of the Union International Contre le Cancer – TNM staging system.[11] Histologic specimens were fixed in 10% formalin and routinely processed for paraffin-embedding. Paraffin-embedded specimens were stored in the dark room in the Department of Pathology of Osaka University Hospital at room temperature, and were sectioned at 4-μm thickness at the time of staining. In some cases, total RNA was extracted using RNeasy kit (Qiagen, Valencia, CA, USA) with DNase I treatment. All patients were followed up with laboratory examinations including routine peripheral blood cell counts at 1- to 6-month intervals, chest roentgenogram, computed tomographic scan of the chest, and endoscopic examinations of the bronchus at 6- to 12-month intervals. The follow-up period for survivors ranged from 5 to154 months (median, 63). The study was approved by the ethical review board of the Graduate

This work is original, and contains no materials previously presented in any reports and publications.

[4]To whom correspondence should be addressed.
E-mail: morii@patho.med.osaka-u.ac.jp

doi: 10.1111/j.1349-7006.2008.01066.x

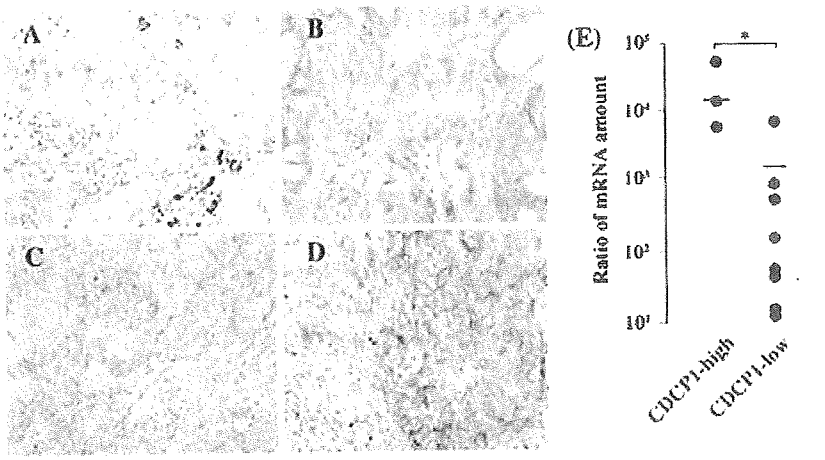

Fig. 1. Surface staining of CDCP1-low (A and B) and -high (C and D) cases, × 400 (E) Real-time reverse transcription–polymerase chain reaction. The amount of CDCP1 mRNA was significantly higher in immunohistochemically defined CDCP1-high cases than in CDCP1-low cases. The bar shows mean values of the amount of CDCP1 mRNA. *$P < 0.01$

Table 1. Summary of characteristics in 200 pulmonary adenocarcinoma patients

Sex	Number of patients
Male	113
Female	87
Tumor size (cm)	
≥5	12
<5	187
Lymph node metastasis	
N0	159
N1	8
N2	29
N3	4
Stage	
I	144
II	19
III	37
Recurrence	
Positive	60
Negative	140
Prognosis	
Dead	41
Alive (with recurrence)	24
Alive (with no recurrence)	135

School of Medicine, Osaka University. Informed consent was obtained from each patient.

Immunohistochemistry for CDCP1, phosphorylated CDCP1 and Ki-67. CDCP1 expression was immunohistochemically examined with use of anti-CDCP1 (Abcam Ltd, Cambridge, UK) and antiphosphorylated CDCP1 antibody. The antiphosphorylated CDCP1 antibody recognizes CDCP1 phosphorylated at Tyr734 and can be used for immunostaining on paraffin-embedded sections.[10,12] The proliferative activity of cancer cells was examined with monoclonal antibody MIB-1 (Immunotech, Marseilles, France), recognizing the proliferation-associated antigen Ki-67. After antigen retrieval with Pascal pressurized heating chamber (Dako, Glostrup, Denmark), the sections were incubated with anti-CDCP1, phosphorylated CDCP1 antibody and MIB-1, diluted at ×200, ×400 and ×100, respectively. Then, the sections were treated with biotin-conjugated antigoat IgG (Zymed, San Francisco, CA, USA) for CDCP1 staining, or with biotin-conjugated antimouse IgG (Dako) for phosphorylated CDCP1 and MIB-1 staining. After washing, the sections were incubated with the peroxidase-conjugated biotin-avidin complex (Vectastain ABC kit, Vector Laboratories, Burlingame, CA, USA), diaminobenzidine (Vector Laboratories) was used as a chromogen. As the negative control, staining was carried out in the absence of a primary antibody. Stained sections were evaluated independently by two pathologists (JI and EM). Generally, CDCP1 expression levels varied among tumor cells in the same case. Staining intensity of tumor cells was divided into four categories; tumor cells with no (representative field was demonstrated in Fig. 1A), weak (Fig. 1B), moderate (Fig. 1C), or strong (Fig. 1D) membrane staining. The intensity of CDCP1 expression in each case was defined by the major population of staining as follows: cases with tumor cells showing no or weak membrane staining were categorized as CDCP1-low, and those showing moderate or strong membrane staining as CDCP1-high. The MIB-1 labeling index was defined as the percentage of stained nuclei per 1000 cells. The cases were divided into MIB-1-high and MIB-1-low groups using the median as cut-off value.

Quantification of mRNA by real-time reverse transcription-polymerase chain reaction (RT-PCR). To evaluate the specificity of CDCP1 immunostaining, expression level of CDCP1 at mRNA and protein levels was compared. For this, fresh frozen materials were available in 13 of the 200 cases. Total RNA was extracted using RNeasy kit (Qiagen, Valencia, CA, USA) with DNase I treatment. Two micrograms of total RNA was subjected to reverse transcription using Superscript III (Invitrogen, Carlsbad, CA, USA). The mRNA levels for CDCP1 and glyceraldehyde-3-phosphate dehydrogenase (GAPDH) genes were verified using TaqMan Gene Expression Assays (Hs00224587_m1 and 4310884E, respectively; Applied Biosystems, Foster City, CA, USA) as recommended by the manufacturer. The amount of CDCP1 mRNA was normalized to that of GAPDH mRNA.

Statistical analysis. Statistical analyses were performed using StatView software (SAS Institute Inc., Cary, NC, USA). The Chi-square and Fisher's exact probability test were used to analyze the correlation between CDCP1 expression and clinicopathological factors in pulmonary adenocarcinoma. Kaplan-Meier methods were used to calculate overall survival (OS) and disease-free survival (DFS) rate, and differences in survival curves were evaluated with the log-rank test. Cox's proportional hazards regression model with a stepwise manner was used to analyze the independent prognostic factors. The *P*-values of less than 0.05 were considered to be statistically significant.

Results

Tumor stages in the present patients were: stage I in 144 patients (72.0%); II in 19 patients (9.5%); and III in 37 patients (18.5%). The histological types of tumors were: bronchioloalveolar

doi: 10.1111/j.1349-7006.2008.01066.x

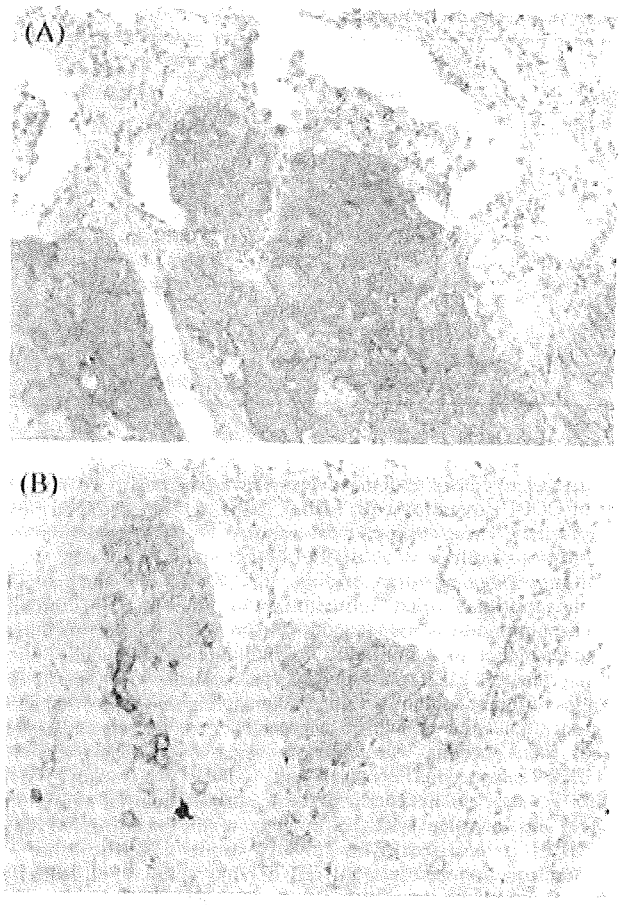

Fig. 2. Localization of phosphorylated CDCP1 in lung adenocarcinoma. Stained cells with anti-CDCP1 antibody (A), and antiphosphorylated CDCP1 antibody (B). Among the CDCP1-positive tumor cells, peripheral areas of tumor cell nests were stained with antiphophorylated CDCP1 antibody. × 400.

(62 patients, 31.0%); papillary (48 patients, 24.0%); or mixed bronchioloalveolar and papillary adenocarcinoma (90 patients, 45.0%). The 5-year DFS and OS was 78.7% and 80.6%, respectively. Tumors recurred in 60 patients. Of these, 38 patients died due to the tumors.

To evaluate the specificity of immunohistochemical staining for CDCP1 expression, quantitative real-time RT-PCR was performed: expression levels of CDCP1 at protein and mRNA level was compared in 13 cases (3 CDCP1-high and 10 CDCP1-low cases at immnohistochemical results). The amount of CDCP1 mRNA was significantly higher in cases with CDCP1-high expression at immunohistochemistry than those with CDCP1-low expression ($P < 0.01$, Fig. 1E). These results showed that the immunohistochemical evaluation is a reliable method for evaluation of CDCP1 expression.

Immunohistochemical detection of CDCP1 expression was carried out in 200 lung adenocarcinoma tissues. Sixty of 200 cases (30.0%) were categorized as CDCP1-high, and the remaining as CDCP1-low. Representative staining results were illustrated in Fig. 1(A–D).

Intracellular tyrosine residues of CDCP1 are known to be phosphorylated upon activation *in vitro*. To examine the localization of activated CDCP1, 43 cases of CDCP1-high lung adenocarcinoma tissues were stained with antiphosphorylated CDCP1. Phosphorylated CDCP1 was detected only in a small portion of CDCP1-expressing cells (Fig. 2 A and 2B), which

Table 2. Correlation between CDCP1 expression and clinicopathological parameters

	CDCP1 expression		*P*
	Low	High	
Tumor size (cm)			
≥5	7	5	
<5	133	55	0.3630
Lymph node metastasis			
N0	120	39	
N1	3	5	
N2	15	14	
N3	2	2	0.0086
Stage			
I	110	34	
II	11	8	
III	19	18	0.0059
MIB-1 labeling index			
≥5%	56	45	
<5%	84	15	<0.0001
Recurrence			
Positive	23	37	
Negative	117	23	<0.0001
Prognosis			
Dead	17	24	
Alive (with recurrence)	10	14	
Alive (with no recurrence)	113	22	<0.0001

appeared to be localized to the peripheral areas of tumor cell nests. Cells without CDCP1 expression did not show any phosphorylated CDCP1 signals, indicating the specificity of the antiphophorylated CDCP1 antibody. Phosphorylated CDCP1 was detected in 19 out of 43 cases: any significant clinicopathological differences were not observed between cases with and without phosphorylated CDCP1.

Correlation of CDCP1 expression with the clinicopathological features was evaluated. Significant positive correlation was observed between CDCP1-high expression and relapse rate ($P < 0.0001$), poor prognosis ($P < 0.0001$), MIB-1 labeling index ($P < 0.0001$), and occurrence of lymph node metastasis ($P = 0.0086$). Other parameters including tumor size and stage did not correlate with CDCP1 expression (Table 2). There was a statistically significant difference in DFS rates ($P < 0.0001$) and OS rates ($P < 0.0001$) between patients with CDCP1-high and CDCP1-low tumors (Fig. 3).

Univariate analysis showed that lymph node status, tumor stage, and CDCP1 expression were significant factors for both OS and DFS (Table 3). The multivariate analysis revealed that only CDCP1 expression was an independent prognostic factor for both OS and DFS.

Discussion

Patient characteristics such as the gender (male preponderance), age distribution (median age, 6th decades of life), and 5-year OS of approximately 80% in the present study were similar to those in a previous report on the lung adenocarcinoma.[13] In addition, the univariate analysis showed the prognostic significance of occurrence of lymph node metastasis and stage of disease, as reported previously.[13] These findings indicate that the results obtained from the present cases are commonly applicable.

Among the clinicopathological factors examined, high CDCP1 expression level correlated with increased occurrence of lymph node metastasis and tumor relapse. A previous study using the lung adenocarcinoma cell lines indicated a significant role of CDCP1 for anchorage-independent growth of tumor cells.[10]

Table 3. Univariate and multivariate analyses of prognostic factors for overall and disease-free survivals

	Overall survival				Disease-free survival			
	Univariate		Multivariate		Univariate		Multivariate	
	HR (95% CI)	*P*-value	HR (95% CI)	*P*-value	HR (95% CI)	*P*-value	HR (95% CI)	*P*-value
Tumor size	1.07 (0.79–1.43)	0.672			1.11 (0.86–1.45)	0.425		
Lymph node status	2.34 (1.77–3.08)	<0.001	1.46 (0.85–2.50)	0.167	2.40 (1.82–3.17)	<0.001	1.43 (0.84–2.40)	0.182
Stage	2.64 (1.90–3.69)	<0.001	1.63 (0.87–3.06)	0.128	2.77 (1.99–3.86)	<0.001	1.74 (0.95–3.20)	0.074
MIB-1 labeling index	1.46 (0.78–2.74)	0.235			1.44 (0.77–2.69)	0.250		
CDCP1 expression	4.11 (2.18–7.75)	<0.001	2.89 (1.51–5.54)	0.001	4.32 (2.31–8.08)	<0.001	3.04 (1.60–5.80)	<0.001

HR, hazard ratio; CI, confidence interval.

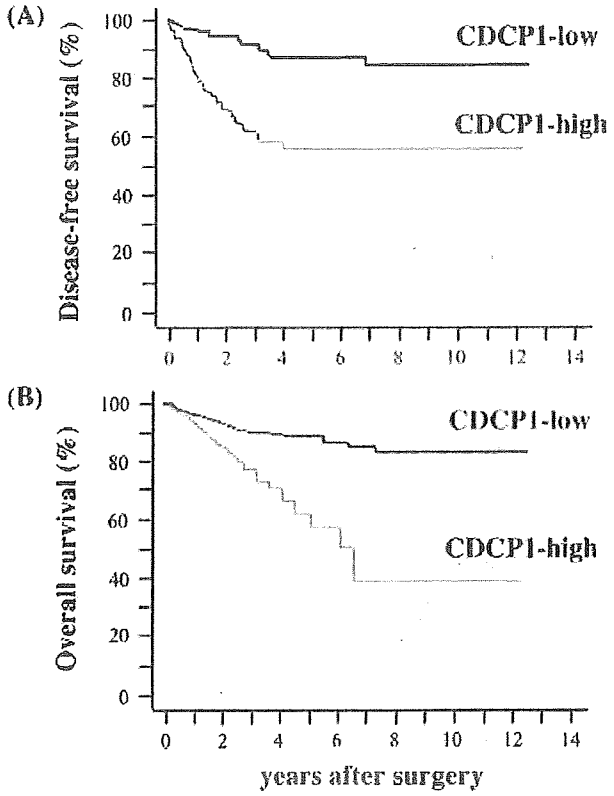

Fig. 3. Kaplan-Meier plots of disease-free (A) and overall survival (B) of patients.

The knocked-down expression of CDCP1 abolished ability of *in vitro* colony formation in the A549 lung adenocarcinoma cell line.[10] In addition, when injected into nude mice, the number of metastatic nodules was low in CDCP1-knocked down A549 cells as compared to parental A549 cells.[10] Taken together with the present results, CDCP1 appeared to play important roles for metastatic and tumorigenic potentials of lung adenocarcinoma not only in cell lines but also in clinical samples.

High CDCP1 expression was correlated with MIB-1 labeling index. Since the monoclonal antibody MIB-1 recognizes Ki-67 antigen that is expressed in cells during the cell cycle, except at the G0 phase, it can be applied to evaluate the proliferative activities of cells. Previously, we showed the positive correlation of CDCP1 expression with MIB-1 labeling index in breast cancer cells.[8] These findings indicate that CDCP1 expression level reflects a proliferative activity of cancer cells.

Intracellular tyrosine residues of CDCP1 are known to be phosphorylated upon activation, and the level of tyrosine phosphorylation is associated with the capacity for anchorage independence in A549 cells.[10] Immunohistochemically, phosphorylated CDCP1 was found to be localized to the peripheral areas of tumor cell nests. Lung adenocarcinoma cells often show bronchioalveolar growth in the periphery of the cancer tissues, but such portions were almost negative for phosphorylated CDCP1 expression. Phosphorylated CDCP1 was mostly present in the tumor cells expanding to the surrounding normal tissues. This was consistent with the previous report that phosphorylated CDCP1 is localized in the invasive front of gastric cancer.[12] Therefore, phosphorylated CDCP1 may play some roles for tumor invasion, in addition to anchorage independence. The staining for phosphorylated and non-phosphorylated CDCP1 demonstrated that most tumor cells expressed CDCP1 as a non-phosphorylated form. This was consistent with the report by Brown *et al.* that the phosphorylation of CDCP1 is dynamically balanced by Src-family kinase and phosphotyrosine phosphatase activities, yielding low equilibrium phosphorylation.[6] CDCP1 contains three extracellular CUB domains, which might be involved in cell adhesion or interaction with the extracellular matrix.[2–7] Non-phosphorylated CDCP1 may function as an adhesion molecule.

Multivariate analysis revealed the high expression of CDCP1 to be an independent factor for poor prognosis for patients with lung adenocarcinoma. Benes *et al.* reported that Src, which mediates proliferation signals in cancers, forms a complex with phosphorylated CDCP1.[7] These findings indicate that overexpression of CDCP1 could stimulate tumor growth, explaining why prognosis of patients with CDCP1-high tumors is worse than that with CDCP1-low tumors.

In conclusion, high CDCP1 expression is an independent factor for poor prognosis of patients with lung adenocarcinoma. Further studies will be necessary to elucidate whether CDCP1 expression could be a useful marker for prediction of prognosis in other types of cancers. CDCP1 could be a molecular target for cancer therapy.

Acknowledgments

The authors thank Ms. Megumi Sugano and Ms. Takako Sawamura for their technical assistance. This work was supported by grants from the Ministry of Education, Culture, Sports, Science and Technology, and from the Osaka Cancer Research Foundation

doi: 10.1111/j.1349-7006.2008.01066.x

References

1 Parkin DM, Bray F, Ferlay J, Pisani P. Global Cancer Statistics, 2002. *CA Cancer J Clin* 2005; **55**: 74–108.

2 Scherl-Mostageer M, Sommergruber W, Abseher R, Hauptmann R, Ambros P, Schweifer N. Identification of a novel gene, CDCP1, overexpressed in human colorectal cancer. *Oncogene* 2001; **20**: 4402–8.

3 Hooper JD, Zijlstra A, Aimes RT *et al.* Subtractive immunization using highly metastatic human tumor cells identifies SIMA135/CDCP1, a 135 kDa cell surface phosphorylated glycoprotein antigen. *Oncogene* 2003; **22**: 1783–94.

4 Conze T, Lammers R, Kuci S *et al.* CDCP1 is a novel marker for hematopoietic stem cells. *Ann NY Acad Sci* 2003; **996**: 222–6.

5 Buhring H J, Kuci S, Conze T *et al.* CDCP1 identifies a broad spectrum of normal and malignant stem/progenitor cell subsets of hematopoietic and nonhematopoietic origin. *Stem Cells* 2004; **22**: 334–43.

6 Brown TA, Yang TM, Zaitsevskaia T *et al.* Adhesion or plasmin regulates tyrosine phosphorylation of a novel membrane glycoprotein p80/gp140/CUB domain-containing protein 1 in epithelia. *J Biol Chem* 2004; **279**: 14713–25.

7 Benes CH, Wu N, Elia AEH, Dharia T, Cantley LC, Soltoff SP. The C2 domain of PKC-delta is a phosphotyrosine binding domain. *Cell* 2005; **121**: 271–80.

8 Ikeda H, Morii E, Kimura H *et al.* Epigenetic regulation of the expression of the novel stem cell marker CDCP1 in cancer cells. *J Pathol* 2006; **210**: 75–84.

9 Kimura H, Morii E, Ikeda H *et al.* Role of DNA methylation for expression of novel stem cell marker CDCP1 in hematopoietic cells. *Leukemia* 2006; **20**: 1551–6.

10 Uekita T, Jia L, Narisawa-Saito M, Yokota J, Kiyono T, Sakai R. CUB domain-containing protein 1 is a novel regulator of anoikis resistance in lung adenocarcinoma. *Mol Cell Biol* 2007; **27**: 7649–60.

11 Sobin LH, Wittekind Ch, eds. *TNM Classification of Malignant Tumors*, 5th edn. New York: John Wiley & Sons, Inc., 1997.

12 Uekita T, Tanaka M, Takigahira M *et al.* CUB domain-containing protein 1 regulates peritoneal dissemination of gastric scirrhous carcinoma. *Am J Pathol* 2008; **172**: 1729–39.

13 Suzuki K, Nagai K, Yoshida J *et al.* Conventional Clinicopathologic Prognostic Factors in Surgically Resected Nonsmall Cell Lung Carcinoma. *Cancer* 1999; **86**: 1976–84.

The American Journal of Pathology, Vol. 175, No. 3, September 2009

DOI: 10.2353/ajpath.2009.090010

Tumorigenesis and Neoplastic Progression

Tumorigenic Role of Orphan Nuclear Receptor NR0B1 in Lung Adenocarcinoma

Tomofumi Oda,*† Tian Tian,* Masayoshi Inoue,† Jun-ichiro Ikeda,* Ying Qiu,*‡ Meinoshin Okumura,† Katsuyuki Aozasa,* and Eiichi Morii*

From the Departments of Pathology and General Thoracic Surgery,† Osaka University, Graduate School of Medicine, Osaka, Japan; and the Department of Pathology,‡ Tongi University School of Medicine, Shanghai, China*

Cancer stem cells are a limited population of tumor cells that are thought to reconstitute whole tumors. The Hoechst dye exclusion assay revealed that tumors are composed of both a main population and a side population of cells, which are rich in cancer stem cells. NR0B1 is an orphan nuclear receptor that is expressed to a greater extent in the side population, as compared with the main population, of a lung adenocarcinoma cell line. In this study, we investigated the role of NR0B1 in lung adenocarcinoma cells. Reduction of NR0B1expression levels in lung adenocarcinoma cell lines resulted in vulnerability to anticancer drugs and decreased abilities for invasion, *in vitro* colony formation, and tumorigenicity in nonobese diabetic/severe compromised immunodeficient mice. When 193 cases of lung adenocarcinoma were immunohistochemically examined, higher levels of NR0B1 expression correlated with higher rates of lymph node metastasis and recurrence. Multivariate analysis revealed high NR0B1 expression levels, stage of the disease, and size of tumor to be independent unfavorable prognostic factors for overall and disease-free survival rates. In clinical samples, NR0B1 expression levels inversely correlated to the proportion of methylated CpG sequences around the transcription initiation site of the NR0B1 gene, suggesting the epigenetic control of NR0B1 transcription in lung adenocarcinoma. In conclusion, NR0B1 might play a role in the malignant potential of lung adenocarcinoma. *(Am J Pathol 2009, 175:1235–1245; DOI: 10.2353/ajpath.2009.090010)*

Cancer cells comprise heterogeneous groups of cells; only a small population of cancer cells possesses the ability to reconstitute whole tumor.[1–3] This population, called cancer stem cells (CSCs), efficiently forms colonies in semisolid culture and is xenotransplantable in non-obese diabetic/severely compromised immunodeficient (NOD/SCID) mice.[4] CSCs were first identified in leukemia,[5,6] and subsequently isolated from the solid tumors, such as breast, brain, prostate, colon, pancreatic, and head/neck cancers.[7–13] CSCs highly express various chemical transporters and could efficiently efflux several chemicals, which might render to resistance to anti-cancer drugs and tumor recurrence.[4,14,15]

Efficient dye-efflux ability could be used for the isolation of CSCs. Most cancer cells are stained intensely with the fluorescent dye Hoechst 33342, whereas cancer cells with stem cell properties are not.[4,14,15] At flow-cytometry analysis, cells with a low level of Hoechst 33342 are visualized as a faintly stained population, which is called the side-population (SP).[16] Only the SP gives rise to both SP and non-SP (the main population, hereafter called MP), and the SP, but not MP, is tumorigenic in NOD/SCID mice.[17] These findings support the notion that CSCs are enriched in the SP. Recently, the presence of SP was reported in cancer cell lines established from various tumors, such as glioma, mammary carcinoma, and lung cancer.[18–20] Proteins highly expressed in the SP may become the candidate of CSC markers.

Lung cancer has become the most common cause of cancer death worldwide since 1985, and the annual mortality was 1.18 million peoples in the world.[21] Despite the advances in the methods for detection and treatment of lung cancer, its prognosis still remains unfavorable. Remnant tumor cells resistant to anti-cancer drugs may provide a basis for recurrence after chemotherapy. In this context, evaluation of lung cancers from the standpoint of CSCs may be important. To date, however, any markers useful for detection of CSCs in lung cancer have not been known. Recently, Seo et al[22] reported that several genes

Supported by grants from the Ministry of Education, Culture, Sports, Science and Technology, Japan.

There is no conflict of interest in this study.

Accepted for publication May 21, 2009.

Address reprint requests to Eiichi Morii, M.D., Department of Pathology, Graduate School of Medicine, Osaka University, Yamada-oka 2-2, Suita 565-0871, Japan. E-mail: morii@patho.med.osaka-u.ac.jp.

were highly expressed in SP of lung adenocarcinoma cell lines: one of them was the gene for NR0B1, a recently characterized member of the orphan nuclear receptor family.[23] NR0B1 (also called dosage-sensitive sex reversal/adrenal hypoplasia congenital critical region on the X chromosome 1; DAX1) acts as a negative regulator of steroid production, and is expressed in the reproductive and endocrine systems.[23] A recent study on the embryonic stem cells showed that NR0B1 is abundantly expressed in an undifferentiated status, but its expression level is down-regulated on differentiation.[24] Knocked down of NR0B1 expression resulted in differentiation of embryonic stem cells, suggesting a role of NR0B1 for the maintenance of undifferentiated state.[25]

NR0B1 is expressed in several kinds of cancers, such as endometrial carcinoma, ovarian carcinoma, prostatic carcinoma, and Ewing's sarcoma.[26–30] Recently, Mendiola et al[29] and Kinsey et al[30] reported that NR0B1 was a target of EWS/FLI fusion protein in Ewing's sarcoma: knocked-down expression of NR0B1 in the Ewing's sarcoma cell lines resulted in the defect of colony formation ability and tumorigenicity. These findings suggested that NR0B1 expression could be a marker for tumorigenic cells in lung adenocarcinoma, as well as Ewing's sarcoma. To date, there have not been any reports describing the expression and role of NR0B1 in lung adenocarcinoma. In the present study, the role of NR0B1 was investigated in lung adenocarcinoma cell line, and subsequently, the clinicopathological features between lung adenocarcinoma with high and low expression level of NR0B1 were compared. In addition, the epigenetic regulation mechanism of NR0B1 gene transcription was investigated.

Materials and Methods

Cells and Flow Cytometry

The human lung adenocarcinoma cell lines A549 and PC-14 were purchased from the American Type Culture Collection (Rockville, MD) and the Riken Bioresource Center (Tsukuba, Japan), respectively. Cells were cultured in Dulbecco's Modified Eagle's Medium (DMEM, Sigma, St Louis, MO) supplemented with 10% fetal calf serum (FCS; Nippon Bio-supp. Center, Tokyo, Japan; DMEM-10% FCS). SP analysis was performed according to the protocol of Goodell's laboratory with minor modifications.[16] Briefly, cells (1×10^6/ml) were incubated at 37°C for 90 minutes with 5 μg/ml Hoechst 33342 (Sigma) with or without 50 μmol/L verapamil (Sigma), collected and resuspended in ice-cold PBS with 2% FCS and 2 μg/ml propidium iodide (BD Pharmingen, San Diego, CA). SP and MP cells were analyzed and sorted with fluorescence-activated cell sorting-Vantage (Becton Dickinson, BD, Franklin Lakes, NJ) carrying a triple-laser. The Hoechst 33342 was excited with the UV laser at 350 nm, and fluorescence emission was measured with 424/BP44 (Hoechst blue) and 660/BP20 (Hoechst red) optical filters.

Quantification of mRNA Levels by Real-Time Reverse-Transcription PCR

RNA was extracted using an RNeasy kit (Qiagen, Valencia, CA) with DNase I treatment. Total RNA was subjected to reverse transcription (RT) by Superscript III (Invitrogen, Carlsbad, CA), and the single strand cDNA was obtained. The mRNA levels for NR0B1, B cell/chronic lymphocytic leukemia lymphoma (Bcl)-2, matrix metalloproteinase (MMP)-2, and glyceraldehyde-3-phosphate dehydrogenase (GAPDH) genes were verified using TaqMan gene expression assays (Applied Biosystems, Foster City, CA) as recommended by the manufacturer. The amount of NR0B1, Bcl-2, and MMP-2 mRNA was normalized to that of GAPDH mRNA, and the normalized value was shown as relative mRNA amount.

Semiquantitative RT-PCR Analysis

The reverse-transcribed product (1 or 0.1 μl) was added to 25 μl of a PCR mixture containing 1.25 U of TaqDNA polymerase (Roche Diagnostics GmbH, Mannheim, Germany) and 25 pmol of each primer. The sequences of the primers were: 5′-CGACTTCGCCGAGATGTCCAGCCAG-3′ and 5′-ACTTGTGGCCCAGATAGGCACCCAG-3′ for Bcl-2, 5′-GGACCCGGTGCCTCAGGA-3′ and 5′-CAAAGATGGTCACGGTCTGC-3′ for BclII-associated x (Bax), 5′-TTGGACAATGGACTGGTTGA-3′ and 5′-GTAGAGTGGATGGTCAGTG-3′ for Bcl-$X_{L/S}$,5′-AGATCTTCTTCTTCAAGGACCGGTT-3′ and 5′-GGCTGGTCAGTGGCTTGGGGTA-3′ for MMP-2, 5′-TTGCGGCCATCTACAGGAG-3′ and 5′-ACTGGGGATCGTTATACATC-3′ for urokinase-type plasminogen activator (uPA), 5′-TGCATGCAGTGTAAGACC-3′ and 5′-CTGCGGCAGATTTTCAAG-3′ for uPA receptor, 5′-ATCCTGTTGTTGCTGTGGCTGATAG-3′ and 5′-TGCTGGGTGGTAACTCTTTATTTCA-3′ for tissue inhibitor of metalloproteinase (TIMP)-1, 5′-TTTATCTACACGGCCCCCTCCTCAG-3′ and 5′-ACGGGTCCTCGATGTCAAGAAACTC-3′ for TIMP-2, and 5′-GTCCACTGGCGTGTTCACCA-3′ and 5′-GTGGCAGTGATGGCATGGAC-3′ for GAPDH.

Knocked Down of NR0B1 Expression by Small Interfering RNA

To generate a stably expressing small interfering (si)-RNA system, the BLOCK-iT Pol II miR RNAi expression vector kit (Invitrogen) was used. Cells stably expressing the NR0B1 si-RNA and control cells stably expressing vector alone were established in DMEM-10% FCS containing blasticidin S (Invivogen) at a concentration of 10 μg/ml in A549 and 12 μg/ml in PC-14.

Immunoblotting

Cells were harvested, and the whole cell lysates were prepared as described previously.[31] The lysates were separated on 10% SDS-polyacrylamide gels, transferred to Immobilon (Millipore, Bedford, MA), and incubated with anti-NR0B1 (Abcam Ltd, Cambridge, UK) or anti-

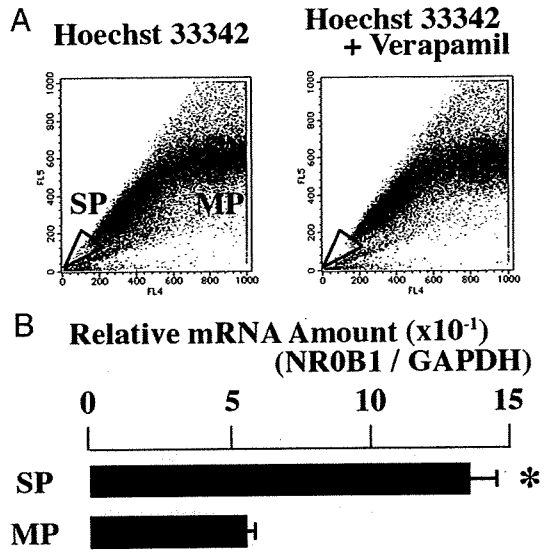

Figure 1. High NR0B1 expression in SP of A549. **A:** Dot blot analysis of A549 cells stained with Hoechst 33342 dye in the absence (**left**) or presence (**right**) of verapamil. SP and MP cells were boxed. **B:** Quantitative real-time RT-PCR was performed with mRNA obtained from SP and MP of A549. The amount of NR0B1 mRNA was normalized for the amount of GAPDH mRNA. The values represent the mean ± SE of three experiments. $^*P < 0.01$ by the Student's *t*-test.

actin (Sigma) antibodies. After washing, the blots were incubated with an appropriate peroxidase-labeled secondary antibody (MBL, Nagoya, Japan), and then reacted with Renaissance reagents (NEN, Boston, MA) before exposure.

Cell Proliferation Assay

Cell growth of A549 was shown by number of cells. Approximately 1 × 10^4 cells were seeded onto cell culture plates with DMEM-10% FCS. The growth medium was changed every 2 days and cell numbers were counted.

Assessment of Anti-Cancer Drug Topotecan Effect

Topotecan acts as a topoisomerase I inhibitor, and induces apoptosis in tumor cells.[32] The effect of topotecan was evaluated as described by Tomicic et al[33] with minor modification. Briefly, cells (1 × 10^4) were seeded onto cell culture plates with DMEM-10% FCS, cultured for 12 hours, and then various concentration of topotecan (LKT Laboratories Inc, St Paul, MN) was added. After 12 hours, the viability of cells was assessed with Premix WST-1 cell assay system (Takara Bio Inc, Kyoto, Japan). The absorbance at 450 nm was divided by that obtained in the cells without topotecan, and the resultant value was shown as viability index.

Matrigel Invasion Assay

Invasion of tumor cells into the Matrigel was examined with BD BioCoat Matrigel Invasion Chamber (BD Biosciences, San Jose, CA). Briefly, cells were seeded in DMEM without FCS on the Matrigel invasion chamber, and cultured in DMEM-10% FCS for 30 hours. Invading cells were stained with Diff-quick staining kit (Siemens, Munich, Germany). Number of invading cells was counted at five microscopic fields per well at a magnification of ×100, and the extent of invasion was expressed as the average number of cells per mm^2.

In Vitro *Colony Formation Assay*

Cells were suspended in a volume of 0.1 ml of DMEM-10% FCS, and 500 cells were plated in culture dishes

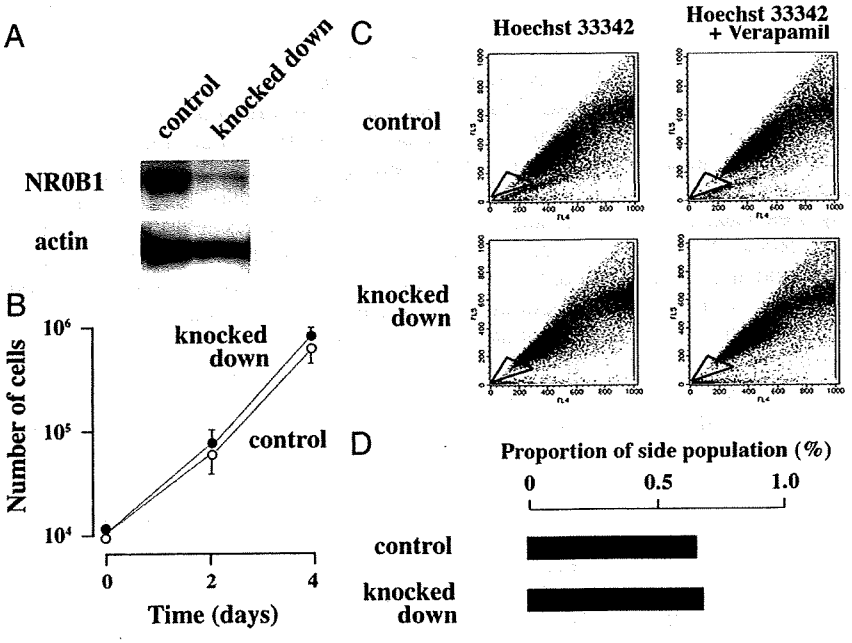

Figure 2. Effect of NR0B1 expression on the proliferative activity and the SP formation. **A:** Immunoblot analysis for the amount of NR0B1 protein in the control and si-RNA knocked down cells. **B:** Comparison of cell proliferation of NR0B1 knocked down cells to that of control cells. The values represent the mean ± SE of three experiments. **C:** Dot blot analysis of control (**upper**) and knocked down (**lower**) cells stained with Hoechst 33342 dye in the absence (**left**) or presence (**right**) of verapamil. SP cells were boxed. **D:** Proportion of SP in the control and knocked down cells.

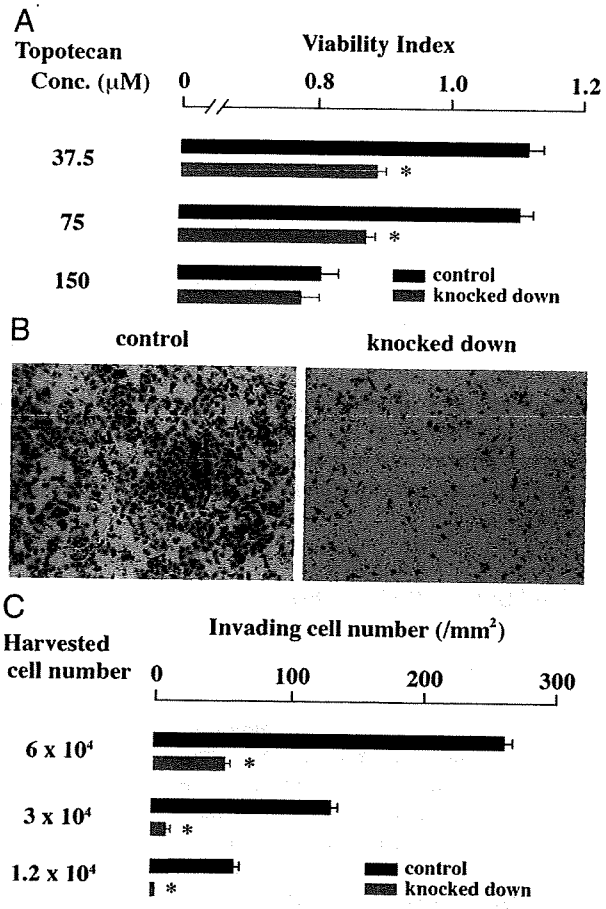

Figure 3. Effect of NR0B1 expression on the resistance against topotecan and the cell invasion activity. **A:** Viability in the presence of various amount of topotecan was compared. **B:** Matrigel invasion assay. Cells invading through Matrigel are shown. Original magnification, ×100. **C:** Invading cell number per mm². The values shown in **(A)** and **(C)** are the mean ± SE of three experiments. $^*P < 0.01$ by the Student's *t*-test.

with 1 ml of methylcellulose-containing DMEM supplemented with 15% FCS. The number of colonies was counted on day14.

Mice and Xenograft Transplantation

Six-to 8-week-old female NOD/SCID mice were purchased from Charles River Laboratories Japan (Kanagawa, Japan) and kept under specific pathogen-free conditions. Before xenotransplantation, the mice were deeply anesthetized. All animal experiments were performed according to the guideline of Osaka University Animal Center, and approved by the institutional review board of committee of animal experiments (No. 753). For xenograft transplantation, cells (1×10^4) were suspended in 0.2 ml of Matrigel (BD Biosciences), and were injected subcutaneously into NOD/SCID mice. The tumor volume was estimated using the following formula: $(\text{width})^2 \times (\text{length})/2$ according to the report by Meyer-Siegler et al.[34]

In Vitro *Methylation*

The luciferase construct that contained promoter region of NR0B1 starting from nt −474[35] was incubated with *Sss*I methylase (New England Biolabs, Beverly, MA) in the presence (methylated) or absence (mock) of *S*-adenosylmethionine, as recommended by the manufacturer. After DNA isolation, 1 μg of the methylated or mock luciferase construct was transiently transfected into A549, together with 0.2 μg of the phRL-TK containing Renilla luciferase gene (Promega, Madison, WI) using Transfast transfection reagent (Promega). Forty-eight hours after transfection, the luciferase activity was measured by Dual Luciferase Reporter Assay Kit (Promega).

Bisulfite Modification and DNA Sequencing Analysis

One μg of genomic DNA was modified with sodium bisulfite using EpiTect Bisulfite Kit (Qiagen), and used for PCR as a template. The PCR reaction mixture contained 1 μl of DNA in a total volume of 25 μl, 2.5 μl of 10× PCR buffer II, 5 μmol/L $MgCl_2$, 250 μmol/L deoxynucleoside triphosphate, 1 μmol/L of each primer, and 1.25units Taq gold. The PCR buffer II, $MgCl_2$, and Taq gold are parts of the AmpliTaq Gold with Gene Amp kit (Applied Biosystems). Sequence of the primers was as follows; 5′-AGGAAAGTGTTTAGGAGTTTTT and 5′-CCTAAAACCTATTTATACCT. The PCR was done at 95°C for 10 minutes, followed by 40 cycles at 95°C for 1 minute, 51°C for 1 minute, and 72°C for 1 minute. In this condition, equal number of clones was obtained for samples with methylated and unmethylated NR0B1 promoter when equal amount of clone was mixed. Amplified PCR fragments were purified with QIAquick gel extraction kit (Qiagen), and was subcloned into pGEM-T Easy vector (Promega). The sequences of the amplified fragments were analyzed using an ABI 3100 sequencer (Applied Biosystems).

Patients

A total of 193 patients who underwent surgery for lung adenocarcinoma at Osaka University Hospital during the period from January 1993 to January 2004 were examined. The histological stage was determined according to the sixth edition of the Union International Contre le Cancer—TNM staging system.[36] Histological specimens were fixed in 10% formalin and routinely processed for paraffin embedding. Paraffin-embedded specimens were stored in the dark room in the Department of Pathology of Osaka University Hospital at room temperature, and were sectioned at 4 μm thickness at the time of staining. All patients were followed up with laboratory examinations including routine peripheral blood cell counts at 1- to 6-month intervals, chest roentgenogram, computed tomographic scan of the chest, and endoscopic examinations of the bronchus at 6- to 12-month intervals. The follow-up period for survivors ranged from 5 to 150 (median, 61) months. The mRNA and genomic DNA were obtained from several tumor samples, and stocked in −80°C. The study was approved by the ethical review board of Graduate School of Medicine, Osaka University (No. 737).

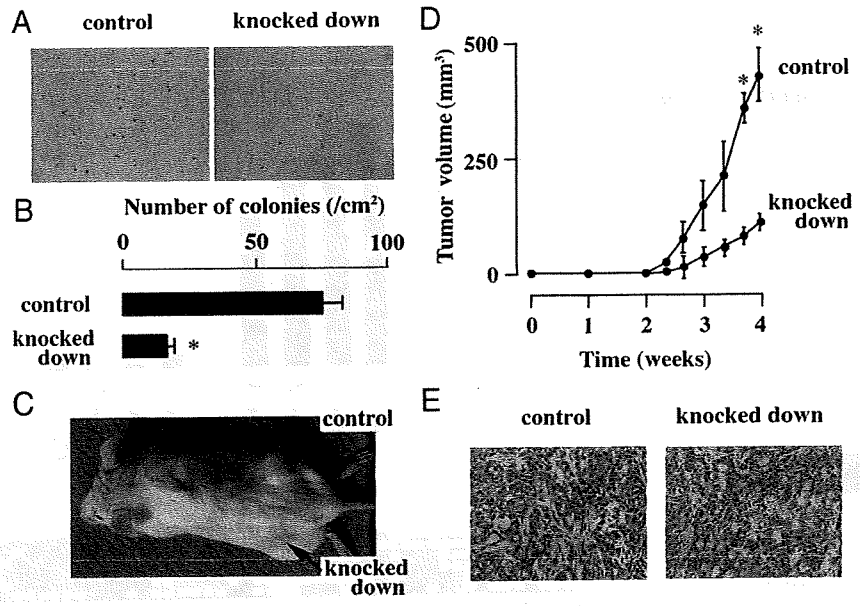

Figure 4. Effect of NR0B1 on the *in vitro* colony formation and the *in vivo* tumorigenicity activities. **A:** Colonies derived from the control and the NR0B1 knocked down cells. Original magnification, ×40. **B:** Number of colonies per cm². **C:** Tumors in NOD/SCID mice at the injection sites of the control and the knocked down cells. **D:** The change of the volume of tumors. **E:** Histology of tumors derived from the control and the knocked down cells. Original magnification, ×400. The values in **(B)** and **(D)** represent the mean ± SE of three experiments. $^*P <$ 0.01 by the Student's *t*-test.

Immunohistochemistry

Immunoperoxidase procedure was performed on the paraffin-embedded sections with standard avidin-biotin-peroxidase complex method. After antigen retrieval with Pascal pressurized heating chamber (DAKO A/S, Glostrup, Denmark), the sections were incubated with anti-NR0B1 (Abcam; 1:100). As the negative control, staining was performed in the absence of primary antibody. Immunohistochemically stained sections were evaluated independently by two investigators (T. O. and E. M.): the results were compared and discussed for patients with discrepant findings.

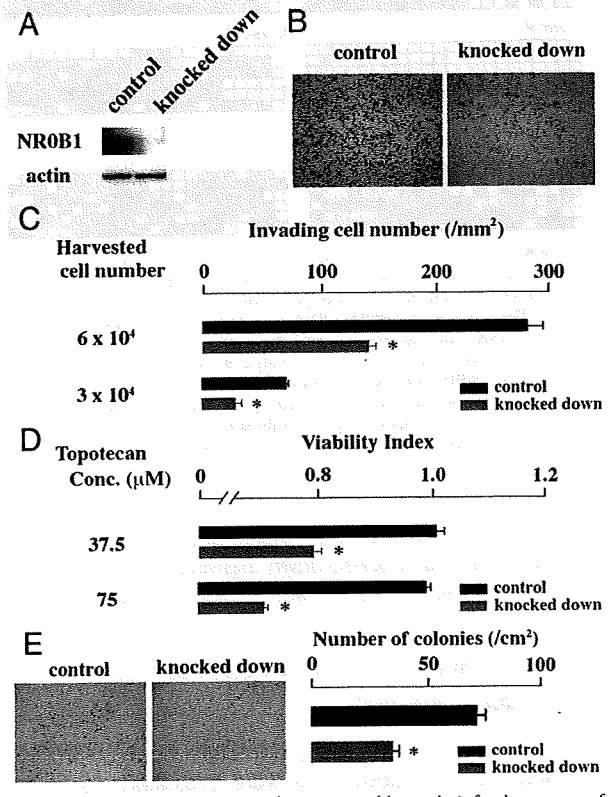

Figure 5. Effect of NR0B1 in PC-14. **A:** Immunoblot analysis for the amount of NR0B1 protein in the control and si-RNA knocked down PC-14 cells. **B:** Matrigel invasion assay using PC-14 cells. Cells invading through Matrigel were shown. Original magnification, ×100. **C:** Invading cell number per mm². **D:** Viability of PC-14 cells in the presence of topotecan was compared. **E:** Colonies derived from the control and the NR0B1 knocked down PC-14 cells, and the number of colonies per cm². The values in **(C)**, **(D)**, and **(E)** represent the mean ± SE of three experiments. $^*P < 0.01$ by the Student's *t*-test.

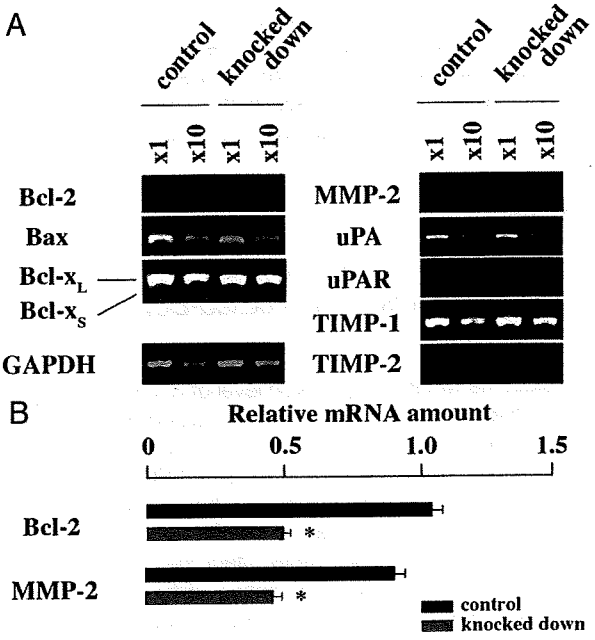

Figure 6. Expression of apoptosis- and invasion-related genes in NR0B1-knocked down A549 cells. **A:** Semiquantitative RT-PCR. **B:** Real-time quantitative RT-PCR to examine the expression level of Bcl-2 and MMP-2. The value is shown as the mean ± SE. $^*P < 0.01$ by the Student's *t*-test.

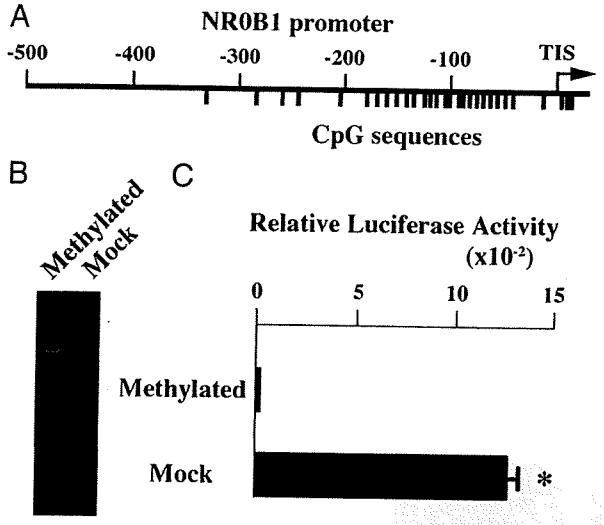

Figure 7. Effect of methylation on NR0B1 promoter activity. **A:** CpG sequences in the NR0B1 promoter. The vertical line represents a single CpG site. Transcription initiation site (TIS) is shown as **arrow**. **B:** Digestion patterns with the methylation-sensitive restriction enzyme HpaII of methylated and mock-methylated reporter plasmids. The luciferase reporter plasmid containing NR0B1 promoter was methylated or mock-methylated *in vitro*. Subsequently, each construct was digested with HpaII and electrophoresed. **C:** Relative luciferase activities of the methylated and mock-methylated NR0B1 constructs. The values represent the mean ± SE of three experiments. $^*P < 0.01$ by the Student's *t*-test. The SE of the methylated construct was too small to be shown.

Statistics

Statistical analysis for experimental studies was performed using Student's *t*-tests. The values are shown as the mean ± SE of at least three experiments. Statistical analysis for clinical samples was performed using StatView software (SAS Institute Inc., Cary, NC). Five-year overall survival (OS) and disease-free survival (DFS) were calculated by the Kaplan-Meier method, and the differences in survival curves were analyzed by the log-lank test. Independent prognostic factors were analyzed by the Cox's proportional hazards regression model.

Results

High Expression Level of NR0B1 in SP of A549 Cells and Effects of its Knocked-Down by si-RNA

To examine whether expression level of NR0B1 was higher in SP than in MP, A549 cells were stained with Hoechst-33342, and the SP and MP were independently sorted (Figure 1A). The expression level of NR0B1 was approximately three times higher in the SP than in the MP (Figure 1B). The expression level of NR0B1 was reduced by si-RNA, but did not significantly affect the proliferative activity and the proportion of SP among A549 cells (Figure 2, A–D). Whereas, the anti-cancer effect of topotecan, which is a topoisomerase I inhibitor and induces apoptosis in tumor cells, was stronger in knocked down cells than in control cells at the concentration of 37.5 and 75 μmol/L (Figure 3A). In Matrigel invasion assay, the number of invading cells in

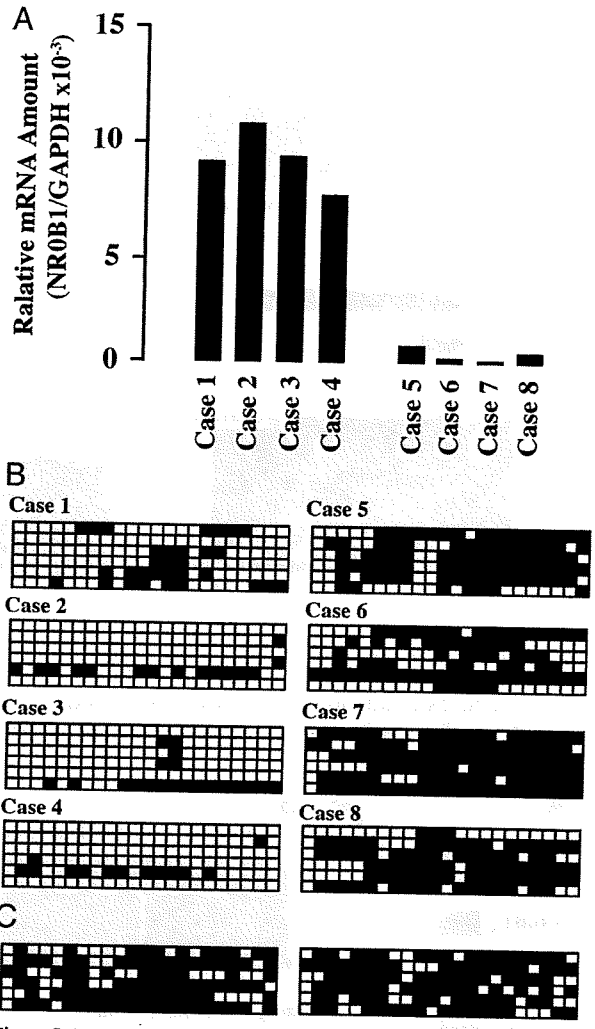

Figure 8. Inverse correlation of NR0B1 expression level to the proportion of methylated CpG sequences in clinical samples of lung adenocarcinoma. **A:** Quantitative real-time RT-PCR was performed with mRNA obtained from tumors. The amount of NR0B1 mRNA was normalized for the amount of GAPDH mRNA. The highest four and the lowest four cases were shown (cases 1 to 4, and cases 5 to 8, respectively). **B:** Methylation status of CpG sequences in NR0B1 promoter. Six clones for each population were analyzed by bisulfite sequencing. Open and closed squares denote unmethylated and methylated cytosines, respectively. **C:** Methylation status of CpG sequences in NR0B1 promoter of normal lung tissue from two cases.

knocked-down cells was lower than that of the control cells, indicating that the knocked-down expression of NR0B1 resulted in a defect of invasive ability (Figure 3, B and C).

Effect of NR0B1 on Colony Formation and Tumorigenic Abilities

The *in vitro* colony formation and *in vivo* tumorigenic activities of NR0B1 knocked-down cells were evaluated. As compared with the control cells, NR0B1 knocked-down cells formed lower number of colonies *in vitro* (Figure 4, A and B). When 1×10^4 cells were injected into NOD/SCID mice, the size of tumors derived from NR0B1 knocked-down cells was significantly smaller than that of control cells (Figure 4, C and D). The tumor derived from either control or knocked-

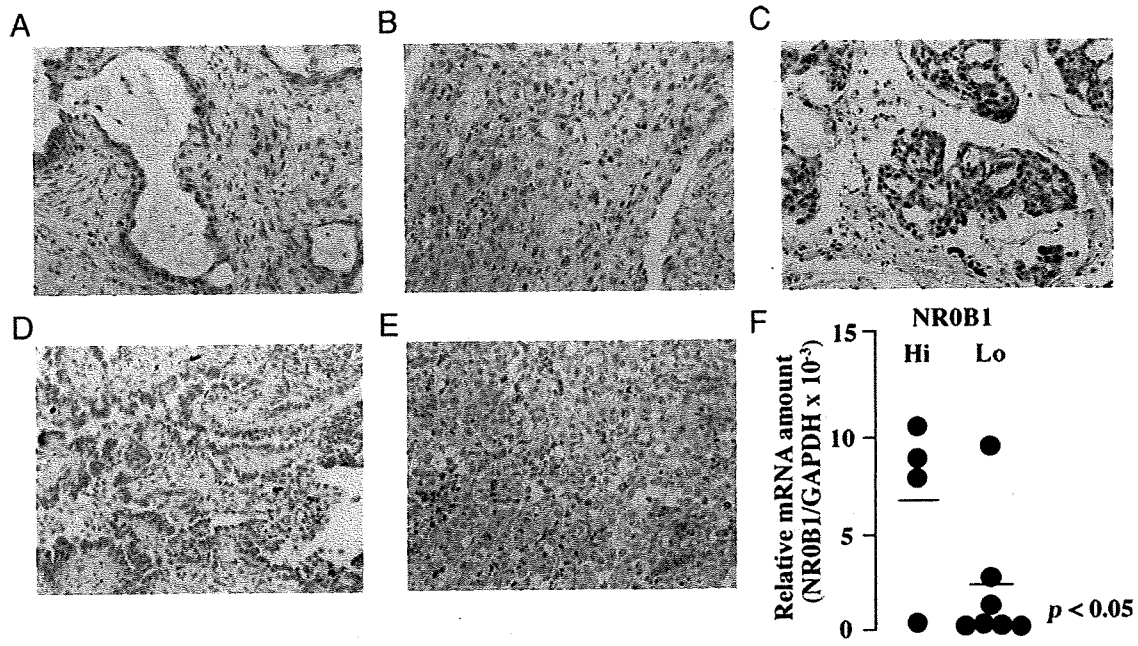

Figure 9. NR0B1 expression in clinical samples of lung adenocarcinoma. **A–E:** Representative pictures of NR0B1 immunostaining in various cases. (×400) NR0B1 signals were detected in the nuclei of approximately 90% (**A**), 70% (**B**), 30% (**C**) of tumor cells. In some cases, the signals were detected not only in the nucleus but also in the cytoplasm (**D**). In other cases, few NR0B1-positive tumor cells were detected (**E**, <1%). **F:** Quantitative real-time RT-PCR was performed with mRNA obtained from 11 tumors as described in Figure 8A. The amount of NR0B1 mRNA was normalized for the amount of GAPDH mRNA. The amount of NR0B1 mRNA was higher in immunohistochemically defined NR0B1-hi cases than in NR0B1-lo cases. The bar shows mean value of NR0B1 amount.

down cells histologically showed glandular structures, mimicking lung adenocarcinoma (Figure 4E).

Effect of NR0B1 in Another Lung Cancer Cell Line

To examine the effect of NR0B1 observed in A549 was applicable to another lung adenocarcinoma cell line, the NR0B1 expression was knocked down in PC-14 (Figure 5A). Matrigel invasion assay revealed that the number of invading cells at NR0B1-knocked down condition reduced to half of the control cells (Figure 5, B and C). The anticancer effect of topotecan was stronger in knocked down cells than in control cells (Figure 5D). In addition, the *in vitro*-formed colony number derived from knocked down cells was smaller than that of control cells (Figure 5E).

Table 1. Brief Summary of 193 Patients with Pulmonary Adenocarcinoma

	No. of patients
Sex	
Male	107
Female	86
T Category	
1	130
2	45
3	13
4	5
N Category	
N0	160
N1	6
N2	24
N3	3
Stage	
I	145
II	18
III	30
Recurrence	
Yes	53
No	140
Prognosis	
Dead	37
Alive (with recurrence)	12
Alive (with no recurrence)	144

Decreased Expression Level of Apoptosis- and Invasion-Related Genes in NR0B1 Knocked-Down Cells

To examine why the colony formation and invasion abilities were defective in NR0B1-knocked down cells, the expression level of apoptosis- and invasion-related genes (Bcl-2, Bax, Bcl-$X_{L/S}$, MMP-2, uPA, uPA receptor, TIMP-1, and TIMP-2) was analyzed. Among the examined genes, Bcl-2 and MMP-2 expression levels were lower in knocked-down cells than in control cells (Figure 6A). Real-time quantitative RT-PCR revealed that the amount of Bcl-2 and MMP-2 mRNAs in knocked down cells decreased to half of control cells (Figure 6B).

Epigenetic Regulation of NR0B1 Expression

A number of CpG sequences were found around the transcription initiation site of NR0B1 gene (Figure 7A), suggesting that the transcription of NR0B1 gene might be epigenetically regulated. To examine this, the luciferase construct containing NR0B1 promoter was methylated *in vitro* using SssI methylase, and the methylated or mock-